

# FRW type Kaluza–Klein modified holographic Ricci dark energy models in Brans–Dicke theory of gravitation

Y. Aditya<sup>1,2,3,a</sup> , D. R. K. Reddy<sup>2,b</sup>

<sup>1</sup> Advanced Analytical Laboratory, Andhra University, Visakhapatnam 530003, India

<sup>2</sup> Department of Applied Mathematics, Andhra University, Visakhapatnam 530003, India

<sup>3</sup> Department of Mathematics, ANITS(A), Visakhapatnam 531162, India

Received: 6 May 2018 / Accepted: 15 July 2018 / Published online: 2 August 2018  
© The Author(s) 2018

**Abstract** In this paper, we investigate non-Ricci, non-compact Friedmann–Robertson–Walker type Kaluza–Klein cosmology in the presence of pressureless matter and modified holographic Ricci dark energy in the frame work of Brans and Dicke (Phys Rev 124:965, 1961) scalar–tensor theory of gravitation. We solve the field equations of this theory using a hybrid expansion law for the five dimensional scale factor. We have also used a power law and a form of logarithmic function of the scale factor for the Brans–Dicke scalar field. Consequently, we obtain two interesting cosmological models of the Kaluza–Klein universe. We have evaluated the cosmological parameters, namely, the equation of state parameter, the deceleration parameter, and the density parameters. To check the stability of our models we use the squared speed of sound. Some well-known cosmological ( $\omega_{de}$ – $\omega'_{de}$  and statefinder) planes are constructed for our models. We have also analyzed the physical behavior of these parameters through graphical representation. It is observed that the FRW type Kaluza–Klein dark energy models presented are compatible with the present day cosmological observations.

## 1 Introduction

The discovery of accelerated expansion of the universe is one of the biggest achievement of the twentieth century [1,2]. A mysterious force with huge negative pressure, dubbed dark energy (DE) was suggested to account for this accelerated expansion. It is also suggested by the WMAP experiment that the universe is composed of 73% DE, 23% dark matter, and 4% baryonic matter [3]. The cosmic expansion of the universe goes through various phases of matter and DE. The DE is normally characterized by the equation of state (EoS)

parameter ( $\omega_{de}$ ) and the ranges include  $-1/3 < \omega_{de} < -1$  for quintessence,  $\omega_{de} = -1$  for the cosmological constant (vacuum), and  $\omega_{de} < -1$  for phantom DE dominated eras.

The cosmological constant cold dark matter ( $\Lambda$ CDM) model is the simplest cosmological model of DE, in which vacuum energy plays the role of DE but it has issues like the coincidence and fine-tuning problems. This motivated various authors to find some alternatives to describe the nature of DE. In this scenario, the matter part of the Einstein–Hilbert action is modified and one proposed various dynamical models such as families of scalar fields (which include quintessence, phantom,  $k$ -essence, etc.) [4–65,67,68], the Chaplygin gas model [8] and holographic DE models [9]. Padmanabhan [10], Copeland et al. [11] and Bamba et al. [12] have presented a comprehensive review of DE models and modified theories of gravity.

The DE problem can be studied in a simpler way using holographic DE (HDE) models [13,14]. In recent years, there has been a lot of interest in HDE models because of the fact that HDE is an emerging model as a candidate of DE constructed by the holographic principle [15]. Motivated by this principle, Cohen et al. [16] recommended that the vacuum energy density is proportional to the Hubble scale i.e.,  $l_H \approx H^{-1}$ . In this model, they successfully explained both the fine-tuning and the coincidence problems, but it is unable to expound the recent cosmic accelerated expansion. The future event horizon has been considered as the characteristic length  $l$  [17]. Later, the inverse of Ricci scalar curvature (i.e.,  $|R|^{-1/2}$ ) has been taken as the length  $l$  [18]; the so-called holographic Ricci DE model. Huang and Li [19] and Zhang and Wu [20] have investigated several properties of holographic Ricci DE. Granda and Oliveros [21] proposed a modified Ricci DE model in which the energy density of DE is a function of the Hubble parameter  $H$  and its first order derivative with respect to cosmic time (i.e.,  $\dot{H}$ ). Chen and Jing [22] have proposed a generalized DE model in which the density of DE

<sup>a</sup> e-mail: yaditya2@gmail.com

<sup>b</sup> e-mail: reddy\_einstein@yahoo.com

contains the second order derivative of Hubble's parameter with respect to time (i.e.,  $\ddot{H}$ ) and is known as modified holographic Ricci DE (MHRDE). This DE model explains the well-known age problem of the old objects. The expression for energy density of MHRDE is defined by Chen and Jing [22] as

$$\rho_{\Lambda} = 3M_p^2(\beta_1 H^2 + \beta_2 \dot{H} + \beta_3 \ddot{H} H^{-1}), \quad (1)$$

where  $M_p^2$  is the reduced Planck mass,  $\beta_1$ ,  $\beta_2$ , and  $\beta_3$  are three arbitrary dimensionless parameters. Some authors have also investigated different DE models in the framework of various theories of gravitation and obtained interesting results [23–32].

The modification in the gravitational part of the Einstein–Hilbert action leads to modified theories of gravitation, and enhancement of dimensions in the original general relativity is another way to handle the DE puzzle. Among the modified theories, the scalar–tensor theories of gravity have got considerable attention. Brans and Dicke (BD) [33] have formulated a scalar–tensor theory where the scalar field  $\phi$  is related with the gravitational constant  $G$  as  $G = \frac{G_0}{\phi}$  and it involves a coupling parameter  $w$ . The scalar field is a fundamental feature of this model of gravity which is considered as a DE candidate. The coupling parameter ( $w$ ) can be adjusted according to the requirement. In particular, in the limit  $w \rightarrow \infty$ , it reduces BD scalar–tensor theory to general relativity.

The study of higher dimensional space-time is an active field of research aimed to unify gravity with other gauge interactions. The concept of extra dimensions is relevant in cosmology, particularly, at the early stage of the universe and theoretically the present four dimensional stage of the universe might have been preceded by a multidimensional stage. This fact has attracted many researchers [34–36] leading them to investigate the cosmological models in the field of higher dimensions. In fact, as time evolves the standard dimensions expand while the extra dimensions shrink to Planckian dimensions, beyond our ability to detect with the currently available experimental facilities [37,38]. Kaluza [39] and Klein [40] have used this extra dimension to unify gravity and electromagnetism in a theory which was essentially five dimensional general relativity. Several authors [41–45] have investigated various cosmological models using five or more dimensions.

The aim of this paper is to obtain non-Ricci, non-compact five dimensional Friedmann–Robertson–Walker (FRW) type Kaluza–Klein (KK) MHRDE models in BD scalar–tensor theory with BD scalar field as power and logarithmic function of the average scale factor. The plan of this paper is as follows. In Sect. 2, we discuss five dimensional FRW space-time, the matter distribution and we formulate the BD field equations. In Sect. 3, we assume a power law and a form of logarithmic

function of the scale factor for the BD scalar field to obtain solutions and analyze the physical behavior of the models obtained. Finally, we conclude our results in the last section.

## 2 Model and field equations

We consider the non-Ricci, non-compact five dimensional FRW type Kaluza–Klein metric in the form

$$ds^2 = dt^2 - a^2 \left\{ \frac{dr^2}{1 - kr^2} + r^2(d\theta^2 + \sin^2 \theta d\phi^2) + (1 - kr^2)d\psi^2 \right\}, \quad (2)$$

where  $a(t)$  is the five dimensional scale factor of the model and  $k = -1, 0, +1$  (curvature parameter,) for open, flat, closed models, respectively. The spatial volume ( $V$ ), Hubble parameter ( $H$ ), expansion scalar ( $\theta$ ) and deceleration parameter ( $q$ ) of this model are given by

$$V = a^4, \quad (3)$$

$$\theta = 4H = 4\frac{\dot{a}}{a}, \quad (4)$$

$$q = \frac{d}{dt} \left( \frac{1}{H} \right) - 1. \quad (5)$$

Several theories have been proposed as alternatives to Einstein's theory. Brans and Dicke [33] formulated a scalar–tensor theory of gravitation which is supposed to be the best alternative to Einstein's theory. We consider the universe filled with pressure-less matter and a modified holographic Ricci DE (MHRDE) fluid. In this case the field equations for the combined scalar and tensor fields given by Brans and Dicke [33] are

$$R_{ij} - \frac{1}{2}Rg_{ij} = -\frac{8\pi}{\phi}(T_{ij} + \bar{T}_{ij}) - \phi^{-1}(\phi_{;i;j} - g_{ij}\phi_{;k}^k) - w\phi^{-2}(\phi_{;i}\phi_{;j} - \frac{1}{2}g_{ij}\phi_{;k}\phi_{;k}), \quad (6)$$

$$\phi_{;k}^k = \frac{8\pi}{(3+2w)}(T + \bar{T}) \quad (7)$$

and the energy conservation equation is

$$(T_{ij} + \bar{T}_{ij})_{;j} = 0, \quad (8)$$

which is a consequence of field equations (6) and (7).

Here  $R$  Ricci scalar,  $R_{ij}$  is Ricci tensor,  $w$  is a dimensionless coupling constant.  $T_{ij}$  and  $\bar{T}_{ij}$  are energy-momentum tensors for pressure-less matter and MHRDE, respectively, which are defined as

$$T_{ij} = \rho_m u_i u_j, \quad (9)$$

$$\bar{T}_{ij} = (\rho_{de} + p_{de})u_i u_j - p_{de}g_{ij}; \quad (10)$$

here  $p_{de}$  and  $\rho_{de}$  are the pressure and energy density of MHRDE, respectively,  $\omega_{de} = p_{de}/\rho_{de}$  is the equation of state (EoS) parameter of MHRDE.  $\rho_m$  is the energy density of matter. The energy density of MHRDE  $\rho_{de}$  is defined by Chen and Jing [22],

$$\rho_{de} = 3M_p^2(\beta_1 H^2 + \beta_2 \dot{H} + \beta_3 \ddot{H} H^{-1}) \tag{11}$$

where  $\beta_1, \beta_2$  and  $\beta_3$  are three arbitrary dimensionless parameters.  $M_p^2 = \frac{1}{8\pi G}$  is the reduced Planck mass and in BD theory  $\phi \propto G^{-1}$ . We have

$$\rho_{de} = \frac{3\phi}{8\pi}(\beta_1 H^2 + \beta_2 \dot{H} + \beta_3 \ddot{H} H^{-1}). \tag{12}$$

By adopting comoving coordinates, the field equations (6) and (7) for the metric (2) using the energy-momentum tensors (9) and (10) yield the following equations:

$$3\frac{\ddot{a}}{a} + 3\frac{\dot{a}^2}{a^2} + 3\frac{k}{a^2} + \frac{w\dot{\phi}^2}{2\phi^2} + 3\frac{\dot{a}\dot{\phi}}{a\phi} + \frac{\ddot{\phi}}{\phi} = -\frac{8\pi}{\phi} p_{de}, \tag{13}$$

$$6\frac{\dot{a}^2}{a^2} + 6\frac{k}{a^2} - \frac{w\dot{\phi}^2}{2\phi^2} + 4\frac{\dot{a}\dot{\phi}}{a\phi} = \frac{8\pi}{\phi}(\rho_{de} + \rho_m), \tag{14}$$

$$\ddot{\phi} + 4\dot{\phi}\frac{\dot{a}}{a} = \frac{8\pi}{3+2w}[\rho_{de} + \rho_m - 4p_{de}], \tag{15}$$

and energy conservation, Eq. (8), leads to

$$\dot{\rho}_{de} + \dot{\rho}_m + 4\frac{\dot{a}}{a}(\rho_{de} + p_{de} + \rho_m) = 0, \tag{16}$$

where the overhead dot denotes ordinary differentiation with respect to time  $t$ .

### 3 Solution of field equations

We can observe that the field equations (13)–(15) are a system of three independent equations with the five unknown parameters  $a, p_{de}, \rho_{de}, \rho_m,$  and  $\phi$ . Hence in order to solve this inconsistent system we need two additional constraints.

Many researchers have used a constant deceleration parameter to obtain the solutions of the model which gives a power law for the metric potentials [46–50]. The positive value of the deceleration parameter represents the early decelerated phase of the universe, whereas the negative value of the deceleration parameter yields the acceleration phase of the universe. Modern observational results from Type Ia supernova and CMB anisotropies suggest that the universe is not only expanding, but also accelerating at present and having decelerated expansion in the past. Therefore, the deceleration parameter must show this transition by its signature changing. That is why the deceleration parameter is variable in time, not a constant. This motivates us to choose the following average scale factor which provides a time dependent deceleration parameter.

The hybrid expansion law (HEL) of the scale factor was initially proposed by Akarsu et al. [51] for Robertson–Walker space-time. Shri Ram and Chandel [52] have investigated the dynamics of a magnetized string cosmological model in  $f(R, T)$  gravity theory using HEL taking

$$a(t) = a_0 t^{\alpha_1} e^{\alpha_2 t}, \text{ where } a_0 > 0. \tag{17}$$

For  $\alpha_1 = 0$  and  $\alpha_2 = 0$ , one can obtain a power-law and exponential expansion from Eq. (17), respectively. When  $\alpha_1$  and  $\alpha_2$  both are non-zero, the universe evolves with variable deceleration parameter.

In the literature it is also common to use a power-law relation between the BD scalar field  $\phi$  and the five dimensional scale factor  $a$  of the form [53, 54]

$$\phi = \phi_0 a^l \tag{18}$$

where  $\phi_0$  is a constant and  $l$  is a power. Many authors have investigated various aspects of this form of the scalar field  $\phi$  and have shown that it leads to a constant deceleration parameter [55, 56] and also to a time varying deceleration parameter [57–59].

Recently, Kumar and Singh [60] proposed a BD scalar field evolving as a logarithmic function of the average scale factor to investigate the evolution of holographic and new agegraphic DE models. The relation is given by

$$\phi = \phi_1 \ln(\eta_1 + \eta_2 a(t)) \tag{19}$$

where  $\phi_1, \eta_1 > 1$  and  $\eta_2 > 0$  are constants. We assume the two forms of scalar field  $\phi$ . Singh and Kumar [61] and Sadri and Vakili [62] have investigated holographic DE models in BD theory using this logarithmic law for scalar field.

#### 3.1 Model 1

Here, we consider a power-law relation between the BD scalar field and the scale factor and find the properties of the model. For this purpose, we assume Eq. (18) to hold.

Substituting the value of average scale factor (17) into Eqs. (13)–(15), (12) and (18), we get the scalar field  $\phi$ ,

$$\phi = \phi_0 (a_0 t^{\alpha_1} e^{\alpha_2 t})^l. \tag{20}$$

##### 3.1.1 Energy densities

The energy density of MHRDE is

$$\rho_{de} = \frac{3\phi_0 (a_0 t^{\alpha_1} e^{\alpha_2 t})^l}{8\pi} \left\{ \beta_1 \left( \frac{\alpha_1}{t} + \alpha_2 \right) - \frac{\beta_2 \alpha_1}{t^2} + \frac{2\beta_3 \alpha_1}{3t^2(\alpha_1 + \alpha_2 t)} \right\}; \tag{21}$$

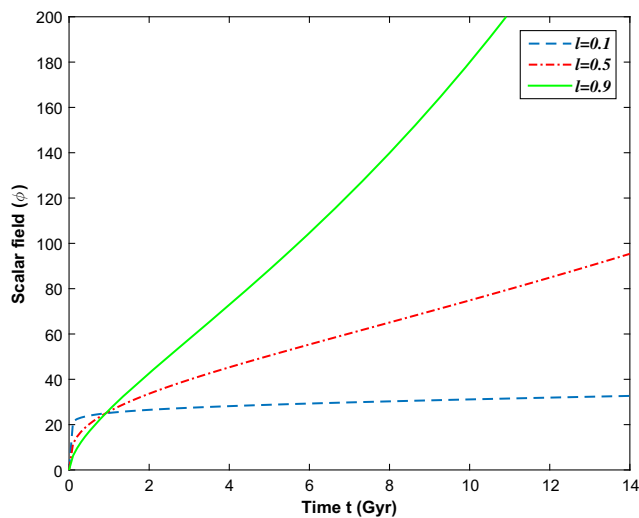


Fig. 1 Plot of scalar field  $\phi$  versus  $t$  in Model 1

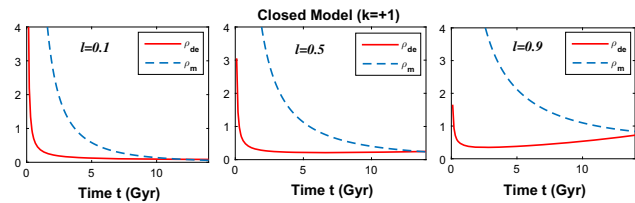


Fig. 2 Plot of energy densities versus cosmic time  $t$  in closed Model 1

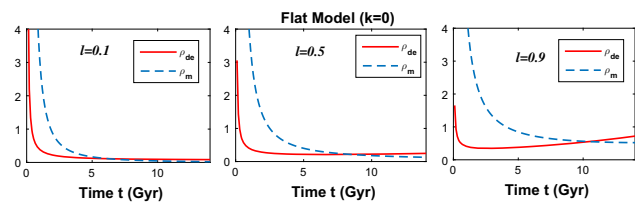


Fig. 3 Plot of energy densities versus cosmic time  $t$  in flat Model 1

the energy density of matter is

$$\rho_m = \frac{\phi_0(a_0 t^{\alpha_1} e^{\alpha_2 t})^l}{8\pi} \left\{ \left( 4l + 6 - \frac{w}{2} l^2 \right) \left( \frac{\alpha_1}{t} + \alpha_2 \right)^2 + \frac{6k}{(a_0 t^{\alpha_1} e^{\alpha_2 t})^2} \right\} - 3 \left\{ \beta_1 \left( \frac{\alpha_1}{t} + \alpha_2 \right) - \frac{\beta_2 \alpha_1}{t^2} + \frac{2\beta_3 \alpha_1}{3t^2(\alpha_1 + \alpha_2 t)} \right\}. \tag{22}$$

It is observed from Fig. 1 that the scalar field increases with time for the different values of  $l = 0.1, 0.5,$  and  $0.9$ . In this section we take the values of the parameters  $\alpha_1 = 0.67, \alpha_2 = 0.065, \beta_1 = 0.2, \beta_2 = 0.48, \beta_3 = 0.5, a_0 = 1, \phi_0 = 25, w = 2,$  and different values of  $l$  i.e.,  $l = 0.1, 0.5, 0.9$ . Figures 2, 3 and 4 represent the energy density of MHRDE and matter (in Model 1) for closed ( $k = +1$ ), flat ( $k = 0$ ) and open ( $k = -1$ ) models with respect to cos-

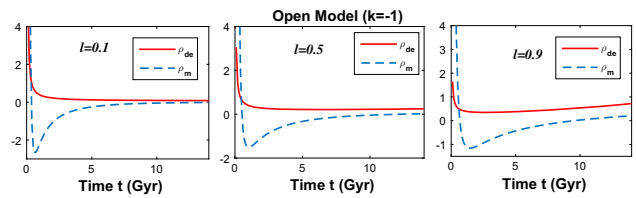


Fig. 4 Plot of energy densities versus cosmic time  $t$  in open Model 1

mic time  $t$ . For the above choice of parameters the energy densities are positive throughout the evolution of the models. It is observed that the energy densities  $\rho_m$  and  $\rho_{de}$  always are positive and decrease with increasing cosmic time in the case of flat and closed models. It can also be observed that the energy density of matter varies in a negative region for the open model, which shows that the open model is not realistic. Furthermore, in the closed and flat models the matter energy density dominates the dark energy density initially and subsequently the dark energy density dominates the matter energy density. Also, it is interesting to note that, as the scalar field increases for different values of  $l$ , the dominance of either the matter energy density or the MHRDE energy density is delayed considerably. Obviously the BD scalar field influences the interaction of the matter energy density and the MHRDE energy density. This is a special feature of our model.

### 3.1.2 Energy conditions

Here we discuss the well-known energy conditions for our MHRDE Model 1. The study of the energy conditions came into existence from the Raychaudhuri equations which play an important role in any discussion of the congruence of null and time-like geodesics. The energy conditions are also the basic tools to prove various general theorems about the behavior of strong gravitational fields. The standard energy conditions are the following:

- Null energy conditions (NEC):  
 $\rho_{\text{eff}} + p_{de} \geq 0,$
- Strong energy conditions (SEC):  
 $\rho_{\text{eff}} + p_{de} \geq 0, \rho_{\text{eff}} + 3p_{de} \geq 0,$
- Weak energy conditions (WEC):  
 $\rho_{\text{eff}} \geq 0, \rho_{\text{eff}} + p_{de} \geq 0,$
- Dominant energy condition (DEC):  
 $\rho_{\text{eff}} \geq 0, \rho_{\text{eff}} \pm p_{de} \geq 0.$

The NEC implies that the energy density of the universe decreases with the expansion and the violation of the NEC may yield a Big Rip of the universe. The violation of the SEC condition represents the accelerated expansion of the universe. The Hawking–Penrose singularity theorems require the validity of SEC and WEC. The WEC and NEC are very

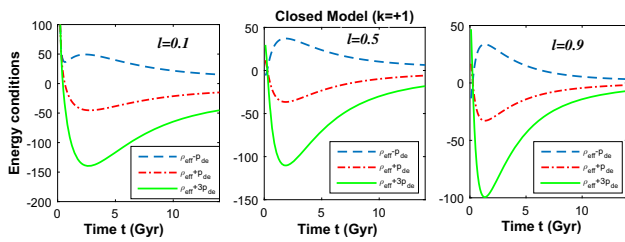


Fig. 5 Plot of energy conditions versus cosmic time  $t$  in closed Model 1

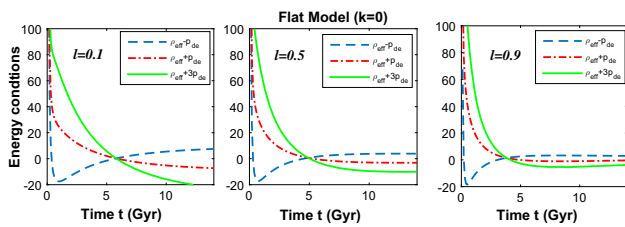


Fig. 6 Plot of energy conditions versus cosmic time  $t$  in flat Model 1

important among all energy conditions as their violation leads to the violation of other energy conditions. Figure 5 presents the energy conditions for different values of  $l$  for closed Model 1. It can be seen that the NEC is violated and hence the model leads to a Big Rip. Also our model violates the SEC, as it should. It can also be seen that the WEC is satisfied. It can also be observed from Fig. 5 that the DEC  $\rho_{\text{eff}} + p_{de}$  is not satisfied. Figure 6 shows the energy conditions in the flat Model 1 for different values of  $l$ . It may be observed that the NEC, SEC, and WEC energy conditions are initially satisfied and are violated at late times. But one of the features of the DEC,  $\rho_{\text{eff}} - p_{de}$ , is initially violated and is satisfied at late times. This is because of the fact that the late time acceleration of the universe is in accordance with the recent observational data.

### 3.1.3 EoS parameter

The EoS parameter of a fluid relates its pressure  $p$  and energy density  $\rho$  by  $\omega = \frac{p}{\rho}$ . Various values of EoS correspond to different epochs of the universe in early decelerating and present accelerating expansion phases. It includes stiff fluid, radiation and matter dominated (dust) for  $\omega = 1$ ,  $\omega = \frac{1}{3}$  and  $\omega = 0$  (decelerating phases), respectively. It represents quintessence  $-1 < \omega < -1/3$ , the cosmological constant  $\omega = -1$  and the phantom case,  $\omega < -1$ .

The EoS parameter of MHRDE  $\omega_{de}$  is

$$\omega_{de} = -\frac{1}{3} \left\{ (l^2 + 3l + 6 + \frac{wl^2}{2}) \left( \frac{\alpha_1}{t} + \alpha_2 \right)^2 + \frac{3k}{(a_0 t^{\alpha_1} e^{\alpha_2 t})^2} - \frac{\alpha_1}{t^2} (l + 3) \right\} \left\{ \beta_1 \left( \frac{\alpha_1}{t} + \alpha_2 \right) - \frac{\beta_2 \alpha_1}{t^2} + \frac{2\beta_3 \alpha_1}{3t^2(\alpha_1 + \alpha_2 t)} \right\}^{-1} \quad (23)$$

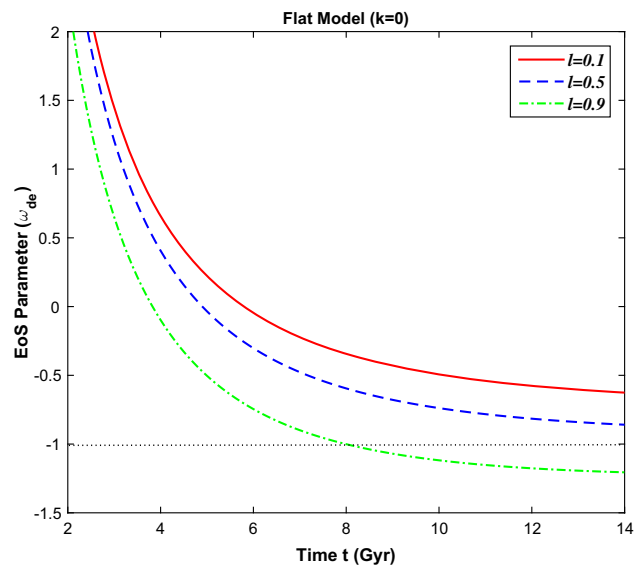


Fig. 7 Plot of EoS parameter versus cosmic time  $t$  in flat Model 1

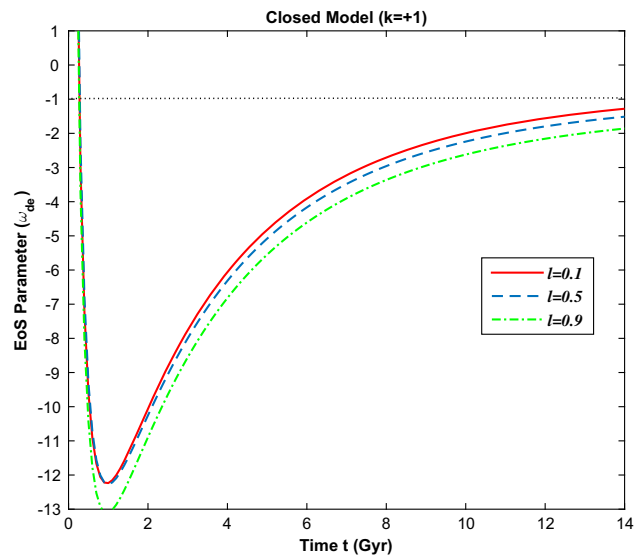


Fig. 8 Plot of EoS parameter versus cosmic time  $t$  in closed Model 1

The EoS parameter of the Model 1 is depicted in Figs. 7 and 8 for different values of  $l$ . It can be seen that, for a flat model ( $k = 0$ ), it starts in the matter dominated era and passes through radiating and dust and attains a constant value in the quintessence region for  $l = 0.1$  and  $0.5$ , while the model crosses the phantom divide line ( $\omega_{de} = -1$ ) and enters into the phantom region. It is interesting to note that as the BD scalar field increases the model approaches the phantom region. Figure 8 depicts the behavior of EoS parameter in the closed Model 1 for different values of the constant  $l$ . In this case it can be observed that the model completely varies in the phantom region and approaches the  $\Lambda$ CDM model at late times.

### 3.1.4 Density parameters

The MHRDE density parameter  $\Omega_{de}$ , matter density parameter  $\Omega_m$ , and total density parameter  $\Omega = \Omega_{de} + \Omega_m + \Omega_k$  are given by

$$\Omega_{de} = \frac{\rho_{de}}{3\phi H^2} = \frac{t^2}{8\pi(\alpha_1 + \alpha_2 t)^2} \left\{ \beta_1 \left( \frac{\alpha_1}{t} + \alpha_2 \right) - \frac{\beta_2 \alpha_1}{t^2} + \frac{2\beta_3 \alpha_1}{3t^2(\alpha_1 + \alpha_2 t)} \right\},$$

$$\Omega_m = \frac{\rho_m}{3\phi H^2} = \frac{t^2}{24\pi(\alpha_1 + \alpha_2 t)^2} \left\{ \left( 4l + 6 - \frac{w}{2} l^2 \right) \times \left( \frac{\alpha_1}{t} + \alpha_2 \right)^2 + \frac{6k}{(a_0 t^{\alpha_1} e^{\alpha_2 t})^2} \right\} - 3 \left\{ \beta_1 \left( \frac{\alpha_1}{t} + \alpha_2 \right) - \frac{\beta_2 \alpha_1}{t^2} + \frac{2\beta_3 \alpha_1}{3t^2(\alpha_1 + \alpha_2 t)} \right\}, \quad (24)$$

$$\Omega_k = \frac{\rho_k}{3\phi H^2} = \frac{k}{a^2 \phi^2}. \quad (25)$$

The overall density parameters for the flat model are presented in Fig. 9 for different values of  $l$ . It is interesting to note that the overall density is constant and  $\approx 1$ . This fact is in agreement with the observational data. It is observed that the matter energy density parameter,  $\Omega_m$ , initially dominates the overall density of dark energy and they interact at a certain point of time. As  $l$  increases it can be noticed that the interaction of the energy densities is being delayed. This is because of the influence of the BD scalar field  $\phi$ . A similar phenomenon may be observed in the flat model given in Fig. 10. It may also be noted that the dark energy density parameter  $\Omega_{de}$  dominates matter energy density parameter. It is well known that dark energy does not directly interact with visible matter except in the rare circumstances. It is quite interesting

that in our case both of them interact at a certain point of time. Figure 10 shows the behavior of the density parameters in the closed model. It can be seen that the overall density parameter approaches the one at very late times, which implies that the model approaches the flat model. It can also be seen that the matter energy density parameter  $\Omega_m$  and the DE density parameter  $\Omega_{de}$  interact at present time.

### 3.1.5 Stability analysis

We now consider an important quantity to verify the stability analysis of MHRDE Model 1 (both closed and flat models). This can be done using the squared speed of sound  $v_s^2$  defined as

$$v_s^2 = \frac{\dot{\rho}_{de}}{\rho_{de}}. \quad (26)$$

A positive value of  $v_s^2$  indicates a stable model whereas a negative value represents a unstable model. We represent  $v_s^2$  of Model 1 (both closed and flat) in Eq. (27) and depict the behavior of  $v_s^2$  in Figs. 11 and 12 for different values of  $l$ . The closed and flat models both are unstable for  $l = 0.1$ . For  $l = 0.5$  the closed model is initially unstable and becomes stable at present epoch; however, for this particular value of  $l$  the flat model initially is unstable, becomes stable, and ultimately attains instability at the present epoch. For  $l = 0.9$ , both models are unstable initially, attain stability for some time, and become unstable at the present epoch. Hence, as the BD scalar field increases, the stability of the Model 1 is different at different times. It may be mentioned here that Myung [63], Jawad et al. [64] and Jawad and Chattopadhyay [65] have performed a stability analysis of DE models

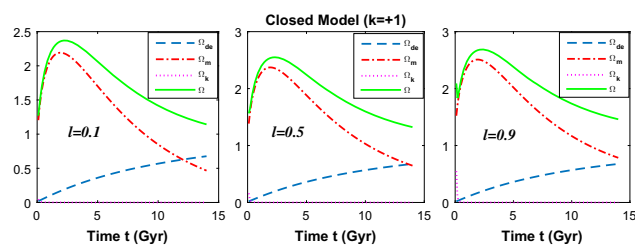


Fig. 9 Plots of density parameters versus  $t$  in closed Model 1

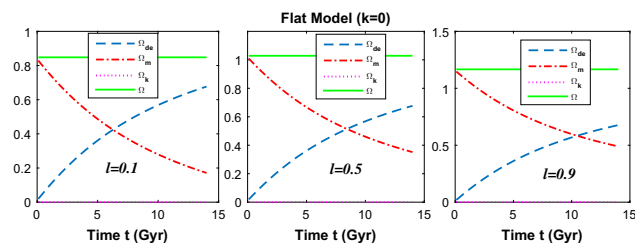


Fig. 10 Plots of density parameters versus  $t$  in flat Model 1

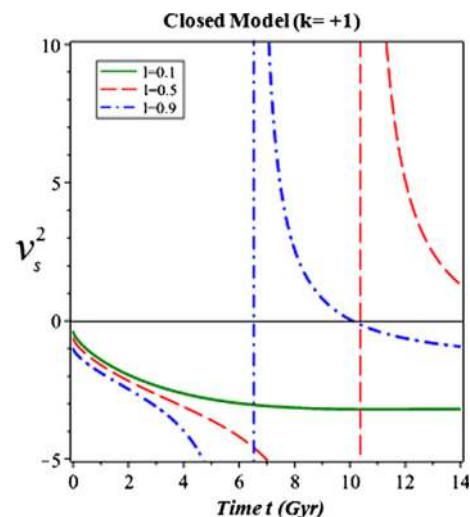
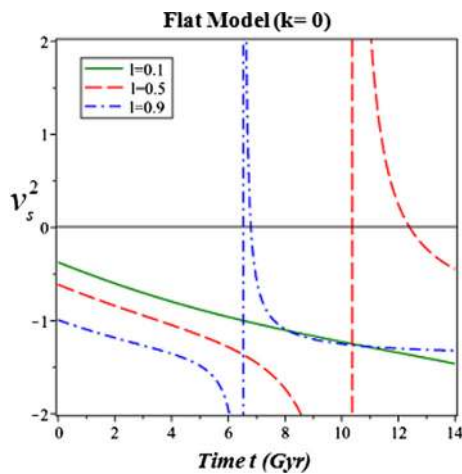


Fig. 11 Plot of  $v_s^2$  versus cosmic time  $t$  for closed Model 1



**Fig. 12** Plot of  $v_s^2$  versus cosmic time  $t$  for flat Model 1

in modified theories of gravitation wherein they have also obtained an unstable behavior of the models. We have

$$\begin{aligned}
 v_s^2 = & \left\{ \frac{-l\phi_0 (a_0 t^{\alpha_1} e^{\alpha_2 t})^l}{24a_0 t^{\alpha_1} e^{\alpha_2 t}} \left\{ \frac{a_0 t^{\alpha_1} \alpha_1 e^{\alpha_2 t}}{t} + a_0 t^{\alpha_1} \alpha_2 e^{\alpha_2 t} \right\} \right. \\
 & \times \left\{ 3 \frac{1}{a_0 t^{\alpha_1} e^{\alpha_2 t}} \left\{ \frac{a_0 t^{\alpha_1} \alpha_1^2 e^{\alpha_2 t}}{t^2} - \frac{a_0 t^{\alpha_1} \alpha_1 e^{\alpha_2 t}}{t^2} \right. \right. \\
 & \left. \left. + 2 \frac{a_0 t^{\alpha_1} \alpha_1 \alpha_2 e^{\alpha_2 t}}{t} + a_0 t^{\alpha_1} \alpha_2^2 e^{\alpha_2 t} \right\} \right. \\
 & \left. + 3 \frac{1}{a_0^2 t^2 \alpha_1 e^2 \alpha_2 t} \left\{ \frac{a_0 t^{\alpha_1} \alpha_1 e^{\alpha_2 t}}{t} + a_0 t^{\alpha_1} \alpha_2 e^{\alpha_2 t} \right\}^2 \right. \\
 & \left. + 3 \frac{k}{a_0^2 t^2 \alpha_1 e^2 \alpha_2 t} + \frac{wl^2}{2a_0^2 t^2 \alpha_1 e^2 \alpha_2 t} \right. \\
 & \times \left\{ \frac{a_0 t^{\alpha_1} \alpha_1 e^{\alpha_2 t}}{t} + a_0 t^{\alpha_1} \alpha_2 e^{\alpha_2 t} \right\}^2 + 3 \frac{l}{a_0^2 t^2 \alpha_1 e^2 \alpha_2 t} \\
 & \times \left\{ \frac{a_0 t^{\alpha_1} \alpha_1 e^{\alpha_2 t}}{t} + a_0 t^{\alpha_1} \alpha_2 e^{\alpha_2 t} \right\}^2 + \frac{1}{\phi_0 (a_0 t^{\alpha_1} e^{\alpha_2 t})^l} \\
 & \times \left\{ \frac{\phi_0 (a_0 t^{\alpha_1} e^{\alpha_2 t})^l l^2}{a_0^2 t^2 \alpha_1 e^2 \alpha_2 t} \left\{ \frac{a_0 t^{\alpha_1} \alpha_1 e^{\alpha_2 t}}{t} + a_0 t^{\alpha_1} \alpha_2 e^{\alpha_2 t} \right\}^2 \right. \\
 & \left. + \frac{\phi_0 (a_0 t^{\alpha_1} e^{\alpha_2 t})^l l}{a_0 t^{\alpha_1} e^{\alpha_2 t}} \left\{ \frac{a_0 t^{\alpha_1} \alpha_1^2 e^{\alpha_2 t}}{t^2} - \frac{a_0 t^{\alpha_1} \alpha_1 e^{\alpha_2 t}}{t^2} \right. \right. \\
 & \left. \left. + 2 \frac{a_0 t^{\alpha_1} \alpha_1 \alpha_2 e^{\alpha_2 t}}{t} + a_0 t^{\alpha_1} \alpha_2^2 e^{\alpha_2 t} \right\} \right. \\
 & \left. - \frac{\phi_0 (a_0 t^{\alpha_1} e^{\alpha_2 t})^l l \alpha_1}{a_0 t^{\alpha_1} e^{\alpha_2 t}} \left\{ \frac{a_0 t^{\alpha_1} \alpha_1 e^{\alpha_2 t}}{t} + a_0 t^{\alpha_1} \alpha_2 e^{\alpha_2 t} \right\} \right. \\
 & \left. - \frac{\phi_0 (a_0 t^{\alpha_1} e^{\alpha_2 t})^l l \alpha_2}{a_0 t^{\alpha_1} e^{\alpha_2 t}} \left\{ \frac{a_0 t^{\alpha_1} \alpha_1 e^{\alpha_2 t}}{t} + a_0 t^{\alpha_1} \alpha_2 e^{\alpha_2 t} \right\} \right\} \\
 & - \frac{\phi_0 (a_0 t^{\alpha_1} e^{\alpha_2 t})^l}{24} \left\{ 3 \frac{1}{a_0 t^{\alpha_1} e^{\alpha_2 t}} \left\{ \frac{a_0 t^{\alpha_1} \alpha_1^3 e^{\alpha_2 t}}{t^3} \right. \right. \\
 & \left. \left. - 3 \frac{a_0 t^{\alpha_1} \alpha_1^2 e^{\alpha_2 t}}{t^3} + 3 \frac{a_0 t^{\alpha_1} \alpha_1^2 \alpha_2 e^{\alpha_2 t}}{t^2} + 2 \frac{a_0 t^{\alpha_1} \alpha_1 e^{\alpha_2 t}}{t^3} \right. \right.
 \end{aligned}$$

$$\begin{aligned}
 & \left. - \frac{3a_0 t^{\alpha_1} \alpha_1 \alpha_2 e^{\alpha_2 t}}{t^2} + 3 \frac{a_0 t^{\alpha_1} \alpha_1 \alpha_2^2 e^{\alpha_2 t}}{t} + a_0 t^{\alpha_1} \alpha_2^3 e^{\alpha_2 t} \right\} \\
 & - 3 \frac{\alpha_1}{a_0 t^{\alpha_1} e^{\alpha_2 t}} \left\{ \frac{a_0 t^{\alpha_1} \alpha_1^2 e^{\alpha_2 t}}{t^2} - \frac{a_0 t^{\alpha_1} \alpha_1 e^{\alpha_2 t}}{t^2} \right. \\
 & \left. + 2 \frac{a_0 t^{\alpha_1} \alpha_1 \alpha_2 e^{\alpha_2 t}}{t} + a_0 t^{\alpha_1} \alpha_2^2 e^{\alpha_2 t} \right\} \\
 & - 3 \frac{\alpha_2}{a_0 t^{\alpha_1} e^{\alpha_2 t}} \left\{ \frac{a_0 t^{\alpha_1} \alpha_1^2 e^{\alpha_2 t}}{t^2} - \frac{a_0 t^{\alpha_1} \alpha_1 e^{\alpha_2 t}}{t^2} \right. \\
 & \left. + 2 \frac{a_0 t^{\alpha_1} \alpha_1 \alpha_2 e^{\alpha_2 t}}{t} + a_0 t^{\alpha_1} \alpha_2^2 e^{\alpha_2 t} \right\} + 6 \frac{1}{a_0^2 t^2 \alpha_1 e^2 \alpha_2 t} \\
 & \times \left\{ \frac{a_0 t^{\alpha_1} \alpha_1 e^{\alpha_2 t}}{t} + a_0 t^{\alpha_1} \alpha_2 e^{\alpha_2 t} \right\} \left\{ \frac{a_0 t^{\alpha_1} \alpha_1^2 e^{\alpha_2 t}}{t^2} \right. \\
 & \left. - \frac{a_0 t^{\alpha_1} \alpha_1 e^{\alpha_2 t}}{t^2} + 2 \frac{a_0 t^{\alpha_1} \alpha_1 \alpha_2 e^{\alpha_2 t}}{t} + a_0 t^{\alpha_1} \alpha_2^2 e^{\alpha_2 t} \right\} \\
 & - \frac{6\alpha_1}{a_0^2 t^2 \alpha_1 e^2 \alpha_2 t} \left\{ \frac{a_0 t^{\alpha_1} \alpha_1 e^{\alpha_2 t}}{t} + a_0 t^{\alpha_1} \alpha_2 e^{\alpha_2 t} \right\}^2 \\
 & - \frac{6\alpha_2}{a_0^2 t^2 \alpha_1 e^2 \alpha_2 t} \left\{ \frac{a_0 t^{\alpha_1} \alpha_1 e^{\alpha_2 t}}{t} + a_0 t^{\alpha_1} \alpha_2 e^{\alpha_2 t} \right\}^2 \\
 & - 6 \frac{k\alpha_1}{a_0^2 t^2 \alpha_1 e^2 \alpha_2 t} - 6 \frac{k\alpha_2}{a_0^2 t^2 \alpha_1 e^2 \alpha_2 t} \\
 & + \frac{wl^2}{a_0^2 t^2 \alpha_1 e^2 \alpha_2 t} \left\{ \frac{a_0 t^{\alpha_1} \alpha_1 e^{\alpha_2 t}}{t} + a_0 t^{\alpha_1} \alpha_2 e^{\alpha_2 t} \right\} \\
 & \times \left\{ \frac{a_0 t^{\alpha_1} \alpha_1^2 e^{\alpha_2 t}}{t^2} - \frac{a_0 t^{\alpha_1} \alpha_1 e^{\alpha_2 t}}{t^2} + 2 \frac{a_0 t^{\alpha_1} \alpha_1 \alpha_2 e^{\alpha_2 t}}{t} \right. \\
 & \left. + a_0 t^{\alpha_1} \alpha_2^2 e^{\alpha_2 t} \right\} - \frac{wl^2 \alpha_1}{a_0^2 t^2 \alpha_1 e^2 \alpha_2 t} \left\{ \frac{a_0 t^{\alpha_1} \alpha_1 e^{\alpha_2 t}}{t} \right. \\
 & \left. + a_0 t^{\alpha_1} \alpha_2 e^{\alpha_2 t} \right\}^2 - \frac{wl^2 \alpha_2}{a_0^2 t^2 \alpha_1 e^2 \alpha_2 t} \left\{ \frac{a_0 t^{\alpha_1} \alpha_1 e^{\alpha_2 t}}{t} \right. \\
 & \left. + a_0 t^{\alpha_1} \alpha_2 e^{\alpha_2 t} \right\}^2 + 6 \frac{l}{a_0^2 t^2 \alpha_1 e^2 \alpha_2 t} \left\{ \frac{a_0 t^{\alpha_1} \alpha_1 e^{\alpha_2 t}}{t} \right. \\
 & \left. + a_0 t^{\alpha_1} \alpha_2 e^{\alpha_2 t} \right\} \left\{ \frac{a_0 t^{\alpha_1} \alpha_1^2 e^{\alpha_2 t}}{t^2} - \frac{a_0 t^{\alpha_1} \alpha_1 e^{\alpha_2 t}}{t^2} \right. \\
 & \left. + 2 \frac{a_0 t^{\alpha_1} \alpha_1 \alpha_2 e^{\alpha_2 t}}{t} + a_0 t^{\alpha_1} \alpha_2^2 e^{\alpha_2 t} \right\} - 6 \frac{l\alpha_1}{a_0^2 t^2 \alpha_1 e^2 \alpha_2 t} \\
 & \times \left\{ \frac{a_0 t^{\alpha_1} \alpha_1 e^{\alpha_2 t}}{t} + a_0 t^{\alpha_1} \alpha_2 e^{\alpha_2 t} \right\}^2 - 6 \frac{l\alpha_2}{a_0^2 t^2 \alpha_1 e^2 \alpha_2 t} \\
 & \times \left\{ \frac{a_0 t^{\alpha_1} \alpha_1 e^{\alpha_2 t}}{t} + a_0 t^{\alpha_1} \alpha_2 e^{\alpha_2 t} \right\}^2 + \frac{1}{\phi_0 (a_0 t^{\alpha_1} e^{\alpha_2 t})^l} \\
 & \times \left\{ \frac{\phi_0 (a_0 t^{\alpha_1} e^{\alpha_2 t})^l l^3}{a_0^3 \left\{ t^{\alpha_1} \right\}^3 \left\{ e^{\alpha_2 t} \right\}^3} \left\{ \frac{a_0 t^{\alpha_1} \alpha_1 e^{\alpha_2 t}}{t} + a_0 t^{\alpha_1} \alpha_2 e^{\alpha_2 t} \right\}^3 \right. \\
 & \left. + \frac{3\phi_0 (a_0 t^{\alpha_1} e^{\alpha_2 t})^l l^2}{a_0^2 t^2 \alpha_1 e^2 \alpha_2 t} \left\{ \frac{a_0 t^{\alpha_1} \alpha_1 e^{\alpha_2 t}}{t} + a_0 t^{\alpha_1} \alpha_2 e^{\alpha_2 t} \right\} \right. \\
 & \left. \times \left\{ \frac{a_0 t^{\alpha_1} \alpha_1^2 e^{\alpha_2 t}}{t^2} - \frac{a_0 t^{\alpha_1} \alpha_1 e^{\alpha_2 t}}{t^2} + 2 \frac{a_0 t^{\alpha_1} \alpha_1 \alpha_2 e^{\alpha_2 t}}{t} \right. \right. \\
 & \left. \left. + a_0 t^{\alpha_1} \alpha_2^2 e^{\alpha_2 t} \right\} - \frac{3\phi_0 (a_0 t^{\alpha_1} e^{\alpha_2 t})^l l^2 \alpha_1}{a_0^2 t^2 \alpha_1 e^2 \alpha_2 t} \left\{ \frac{a_0 t^{\alpha_1} \alpha_1 e^{\alpha_2 t}}{t} \right. \right.
 \end{aligned}$$







$$\begin{aligned}
 & \times \left\{ \frac{a_0 t^{\alpha_1} \alpha_1 e^{\alpha_2 t}}{t} + a_0 t^{\alpha_1} \alpha_2 e^{\alpha_2 t} \right\} - \frac{l}{\phi_0 (a_0 t^{\alpha_1} e^{\alpha_2 t})^{l+1}} \\
 & \times \left\{ \frac{\phi_0 (a_0 t^{\alpha_1} e^{\alpha_2 t})^l l^2}{a_0^2 t^{2\alpha_1} e^{2\alpha_2 t}} \left\{ \frac{a_0 t^{\alpha_1} \alpha_1 e^{\alpha_2 t}}{t} + a_0 t^{\alpha_1} \alpha_2 e^{\alpha_2 t} \right\}^2 \right. \\
 & + \frac{\phi_0 (a_0 t^{\alpha_1} e^{\alpha_2 t})^l l}{a_0 t^{\alpha_1} e^{\alpha_2 t}} \left\{ \frac{a_0 t^{\alpha_1} \alpha_1^2 e^{\alpha_2 t}}{t^2} - \frac{a_0 t^{\alpha_1} \alpha_1 e^{\alpha_2 t}}{t^2} \right. \\
 & + 2 \frac{a_0 t^{\alpha_1} \alpha_1 \alpha_2 e^{\alpha_2 t}}{t} + a_0 t^{\alpha_1} \alpha_2^2 e^{\alpha_2 t} \left. \right\} - \frac{\phi_0 (a_0 t^{\alpha_1} e^{\alpha_2 t})^l l \alpha_1}{a_0 t^{\alpha_1} e^{\alpha_2 t} t} \\
 & \times \left\{ \frac{a_0 t^{\alpha_1} \alpha_1 e^{\alpha_2 t}}{t} + a_0 t^{\alpha_1} \alpha_2 e^{\alpha_2 t} \right\} - \frac{\phi_0 (a_0 t^{\alpha_1} e^{\alpha_2 t})^l l \alpha_2}{a_0 t^{\alpha_1} e^{\alpha_2 t}} \\
 & \times \left\{ \frac{a_0 t^{\alpha_1} \alpha_1 e^{\alpha_2 t}}{t} + a_0 t^{\alpha_1} \alpha_2 e^{\alpha_2 t} \right\} \left\{ \frac{a_0 t^{\alpha_1} \alpha_1 e^{\alpha_2 t}}{t} \right. \\
 & + a_0 t^{\alpha_1} \alpha_2 e^{\alpha_2 t} \left. \right\} + \left\{ \frac{3}{a_0 t^{\alpha_1} e^{\alpha_2 t}} \left\{ \frac{a_0 t^{\alpha_1} \alpha_1^2 e^{\alpha_2 t}}{t^2} \right. \right. \\
 & - \frac{a_0 t^{\alpha_1} \alpha_1 e^{\alpha_2 t}}{t^2} + \frac{2a_0 t^{\alpha_1} \alpha_1 \alpha_2 e^{\alpha_2 t}}{t} + a_0 t^{\alpha_1} \alpha_2^2 e^{\alpha_2 t} \left. \right\} \\
 & + \frac{3}{a_0^2 t^{2\alpha_1} e^{2\alpha_2 t}} \left\{ \frac{a_0 t^{\alpha_1} \alpha_1 e^{\alpha_2 t}}{t} + a_0 t^{\alpha_1} \alpha_2 e^{\alpha_2 t} \right\}^2 \\
 & + \frac{3k}{a_0^2 t^{2\alpha_1} e^{2\alpha_2 t}} + \frac{wl^2}{2a_0^2 t^{2\alpha_1} e^{2\alpha_2 t}} \left\{ \frac{a_0 t^{\alpha_1} \alpha_1 e^{\alpha_2 t}}{t} \right. \\
 & + a_0 t^{\alpha_1} \alpha_2 e^{\alpha_2 t} \left. \right\}^2 + \frac{3l}{a_0^2 t^{2\alpha_1} e^{2\alpha_2 t}} \left\{ \frac{a_0 t^{\alpha_1} \alpha_1 e^{\alpha_2 t}}{t} \right. \\
 & + a_0 t^{\alpha_1} \alpha_2 e^{\alpha_2 t} \left. \right\}^2 + \frac{1}{\phi_0 (a_0 t^{\alpha_1} e^{\alpha_2 t})^l} \left\{ \frac{\phi_0 (a_0 t^{\alpha_1} e^{\alpha_2 t})^l l^2}{a_0^2 t^{2\alpha_1} e^{2\alpha_2 t}} \right. \\
 & \times \left\{ \frac{a_0 t^{\alpha_1} \alpha_1 e^{\alpha_2 t}}{t} + a_0 t^{\alpha_1} \alpha_2 e^{\alpha_2 t} \right\}^2 + \frac{\phi_0 (a_0 t^{\alpha_1} e^{\alpha_2 t})^l l}{a_0 t^{\alpha_1} e^{\alpha_2 t}} \\
 & \times \left\{ \frac{a_0 t^{\alpha_1} \alpha_1^2 e^{\alpha_2 t}}{t^2} - \frac{a_0 t^{\alpha_1} \alpha_1 e^{\alpha_2 t}}{t^2} + 2 \frac{a_0 t^{\alpha_1} \alpha_1 \alpha_2 e^{\alpha_2 t}}{t} \right. \\
 & + a_0 t^{\alpha_1} \alpha_2^2 e^{\alpha_2 t} \left. \right\} - \frac{\phi_0 (a_0 t^{\alpha_1} e^{\alpha_2 t})^l l \alpha_1}{a_0 t^{\alpha_1} e^{\alpha_2 t} t} \left\{ \frac{a_0 t^{\alpha_1} \alpha_1 e^{\alpha_2 t}}{t} \right. \\
 & + a_0 t^{\alpha_1} \alpha_2 e^{\alpha_2 t} \left. \right\} - \frac{\phi_0 (a_0 t^{\alpha_1} e^{\alpha_2 t})^l l \alpha_2}{a_0 t^{\alpha_1} e^{\alpha_2 t}} \left\{ \frac{a_0 t^{\alpha_1} \alpha_1 e^{\alpha_2 t}}{t} \right. \\
 & + a_0 t^{\alpha_1} \alpha_2 e^{\alpha_2 t} \left. \right\} \left\{ \frac{\phi_0 (a_0 t^{\alpha_1} e^{\alpha_2 t})^l l}{8a_0 t^{\alpha_1} e^{\alpha_2 t}} \left\{ \frac{a_0 t^{\alpha_1} \alpha_1 e^{\alpha_2 t}}{t} \right. \right. \\
 & + a_0 t^{\alpha_1} \alpha_2 e^{\alpha_2 t} \left. \right\} \left\{ \beta_1 \left\{ \frac{\alpha_1}{t} + \alpha_2 \right\} - \frac{\beta_2 \alpha_1}{t^2} + \frac{2\beta_3 \alpha_1}{t^3} \right. \\
 & \times \left. \left\{ \frac{\alpha_1}{t} + \alpha_2 \right\}^{-1} \right\} + \frac{\phi_0}{8} (a_0 t^{\alpha_1} e^{\alpha_2 t})^l \left\{ -\frac{\beta_1 \alpha_1}{t^2} + 2 \frac{\beta_2 \alpha_1}{t^3} \right. \\
 & + 2 \frac{\beta_3 \alpha_1^2}{t^5} \left\{ \frac{\alpha_1}{t} + \alpha_2 \right\}^{-2} - \frac{6\beta_3 \alpha_1}{t^4} \left\{ \frac{\alpha_1}{t} + \alpha_2 \right\}^{-1} \left. \right\} \\
 & \times \left\{ 3\beta_1 \left\{ \frac{\alpha_1}{t} + \alpha_2 \right\} - 3 \frac{\beta_2 \alpha_1}{t^2} + 6 \frac{\beta_3 \alpha_1}{t^3} \left\{ \frac{\alpha_1}{t} + \alpha_2 \right\}^{-1} \right\}^{-1} \\
 & \times \left\{ \frac{\alpha_1}{t} + \alpha_2 \right\}^{-1} \left\{ \beta_1 \left\{ \frac{\alpha_1}{t} + \alpha_2 \right\} - \frac{\beta_2 \alpha_1}{t^2} \right. \\
 & + 2 \frac{\beta_3 \alpha_1}{t^3} \left\{ \frac{\alpha_1}{t} + \alpha_2 \right\}^{-1} \left. \right\}^{-1}. \tag{28}
 \end{aligned}$$

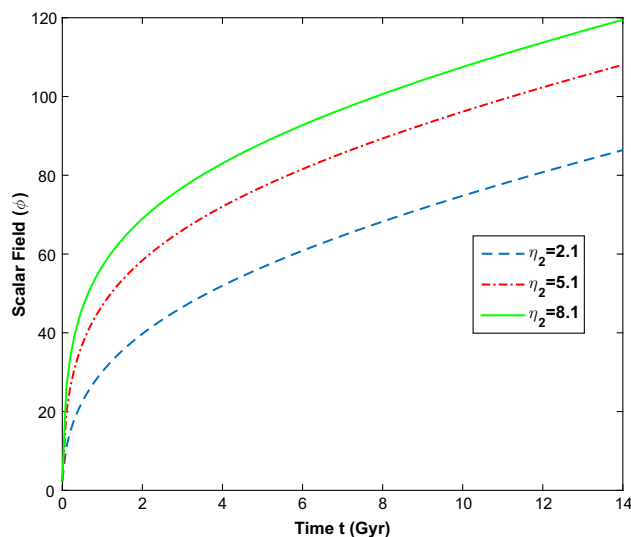


Fig. 15 Plot of scalar field  $\phi$  versus  $t$  in Model 2

### 3.2 Model 2

Here we assume that the scalar field evolves as a logarithmic function of the scale factor and is given by Eq. (19). Substituting the value of average scale factor (17) into Eqs. (13)–(15), (12) and (19), we get the scalar field  $\phi$ ,

$$\phi = \phi_1 \ln [\eta_1 + \eta_2 (a_0 t^{\alpha_1} e^{\alpha_2 t})]. \tag{29}$$

The behavior of BD scalar field of Model 2 is shown in Fig. 15 for different values of  $\eta_2$ . This shows that the scalar field increases as  $\eta_2$  increases.

#### 3.2.1 Energy densities

The energy density of MHRDE is

$$\begin{aligned}
 \rho_{de} = & \frac{3\phi_1 \ln [\eta_1 + \eta_2 (a_0 t^{\alpha_1} e^{\alpha_2 t})]}{8\pi} \left\{ \beta_1 \left( \frac{\alpha_1}{t} + \alpha_2 \right) \right. \\
 & \left. - \frac{\beta_2 \alpha_1}{t^2} + \frac{2\beta_3 \alpha_1}{3t^2 (\alpha_1 + \alpha_2 t)} \right\}, \tag{30}
 \end{aligned}$$

the energy density of matter is

$$\begin{aligned}
 \rho_m = & \frac{\phi_1 \ln (\eta_1 + \eta_2 (a_0 t^{\alpha_1} e^{\alpha_2 t}))}{8\pi} \left\{ \left( \frac{\alpha_1}{t} + \alpha_2 \right)^2 \right. \\
 & \left( 6 - \frac{w\eta_2^2 (a_0 t^{\alpha_1} e^{\alpha_2 t})^2}{2 [(\eta_1 + \eta_2 (a_0 t^{\alpha_1} e^{\alpha_2 t})) \ln (\eta_1 + \eta_2 (a_0 t^{\alpha_1} e^{\alpha_2 t}))]^2} \right) \\
 & + \frac{6k}{(a_0 t^{\alpha_1} e^{\alpha_2 t})^2} \left. \right\} - 3 \left\{ \beta_1 \left( \frac{\alpha_1}{t} + \alpha_2 \right) \right. \\
 & \left. - \frac{\beta_2 \alpha_1}{t^2} + \frac{2\beta_3 \alpha_1}{3t^2 (\alpha_1 + \alpha_2 t)} \right\}. \tag{31}
 \end{aligned}$$

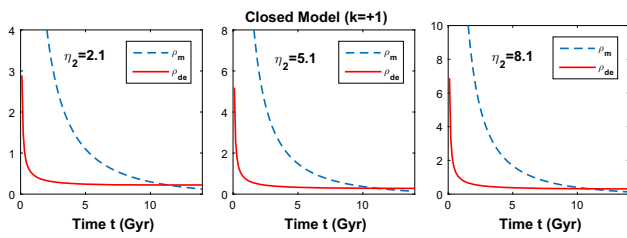


Fig. 16 Plot of energy densities versus cosmic time  $t$  in closed Model 2

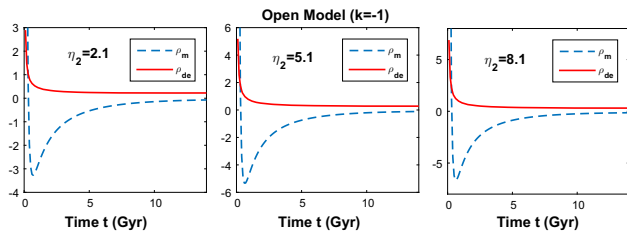


Fig. 17 Plot of energy densities versus cosmic time  $t$  in open Model 2

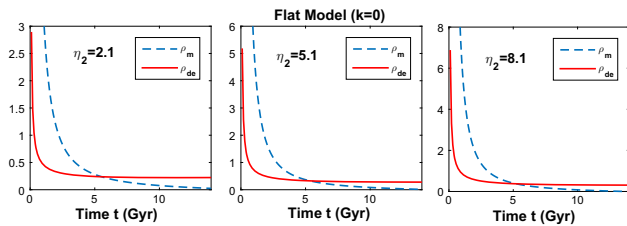


Fig. 18 Plot of energy densities versus cosmic time  $t$  in flat Model 2

The variation of energy densities with time  $t$  for  $\eta_1 = 1.1$  and for different values of  $\eta_2$  is shown in Figs. 16, 17 and 18. The other constants are the same as in Model 1. In this case we observe a similar behavior for flat and closed models to Model 1. However, in this case we see that the dark energy density dominates the matter density earlier than in Model 1. Also as  $\eta_2$  increases the interaction of the energy densities occurs at early times. That is, the increase in the BD scalar field influences the interaction of energy densities. It can also be seen that the open model is not realistic because of the fact that the energy density of matter is negative.

### 3.2.2 Energy conditions

Figures 19, 20 describe the energy conditions of both closed and flat Models 2 for different values of  $\eta_2$ . It can be seen that the validity of the energy conditions for Model 2 is similar to that of the energy conditions of the Model 1.

### 3.2.3 EoS parameter

The EoS parameter of MHRDE,  $\omega_{de}$ , is

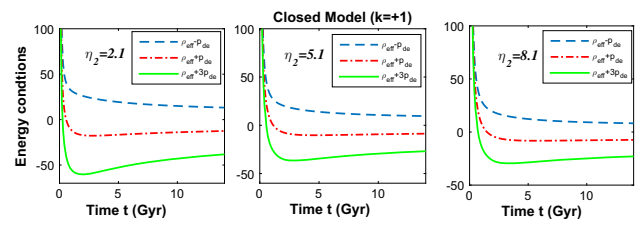


Fig. 19 Plot of energy conditions versus cosmic time  $t$  in closed Model 2

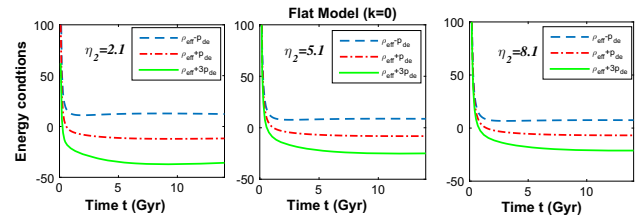


Fig. 20 Plot of energy conditions versus cosmic time  $t$  in flat Model 2

$$\begin{aligned} \omega_{de} = & -\frac{1}{3} \left\{ 6 \left( \frac{\alpha_1}{t} + \alpha_2 \right)^2 + \frac{3k}{(a_0 t^{\alpha_1} e^{\alpha_2 t})^2} - \frac{3\alpha_1}{t^2} \right. \\ & + \frac{\eta_2 (a_0 t^{\alpha_1} e^{\alpha_2 t})^2 \left( \frac{w}{2} + 3l\eta_2 \right) \left( \frac{\alpha_1}{t} + \alpha_2 \right)^2}{\left[ (\eta_1 + \eta_2 (a_0 t^{\alpha_1} e^{\alpha_2 t})) \ln(\eta_1 + \eta_2 (a_0 t^{\alpha_1} e^{\alpha_2 t})) \right]^2} \\ & + (a_0 t^{\alpha_1} e^{\alpha_2 t}) \eta_2 \left\{ (\eta_1 + \eta_2 (a_0 t^{\alpha_1} e^{\alpha_2 t})) \left\{ \frac{\alpha_1 (\alpha_1 - 1)}{t^2} \right. \right. \\ & + \left. \left. \frac{2\alpha_1 \alpha_2}{t} + \alpha_1 \right\}^2 - \eta_2 (a_0 t^{\alpha_1} e^{\alpha_2 t}) \left( \frac{\alpha_1}{t} + \alpha_2 \right)^2 \right\} \\ & \times \left\{ \left[ (\eta_1 + \eta_2 (a_0 t^{\alpha_1} e^{\alpha_2 t}))^2 \ln(\eta_1 + \eta_2 (a_0 t^{\alpha_1} e^{\alpha_2 t})) \right]^{-1} \right\} \\ & \times \left. \left\{ \beta_1 \left( \frac{\alpha_1}{t} + \alpha_2 \right) - \frac{\beta_2 \alpha_1}{t^2} + \frac{2\beta_3 \alpha_1}{3t^2 (\alpha_1 + \alpha_2 t)} \right\}^{-1} \right\}. \quad (32) \end{aligned}$$

The plot of EoS parameter given in Figs. 21, 22 for different values of  $\eta_2$  shows that the flat and closed models completely vary in the phantom region. It is interesting to see that in both models it varies completely in the phantom region.

### 3.2.4 Energy density parameters

The MHRDE density parameter  $\Omega_{de}$ , the matter density parameter  $\Omega_m$ , and the total density parameter  $\Omega$  are given by

$$\begin{aligned} \Omega_{de} = & \frac{3t^2}{8\pi (\alpha_1 + \alpha_2 t)^2} \left\{ \beta_1 \left( \frac{\alpha_1}{t} + \alpha_2 \right) - \frac{\beta_2 \alpha_1}{t^2} \right. \\ & \left. + \frac{2\beta_3 \alpha_1}{3t^2 (\alpha_1 + \alpha_2 t)} \right\}, \\ \Omega_m = & \frac{t^2}{8\pi (\alpha_1 + \alpha_2 t)^2} \left\{ \left( \frac{\alpha_1}{t} + \alpha_2 \right)^2 \right. \\ & \times \left. \left( 6 - \frac{w\eta_2^2 (a_0 t^{\alpha_1} e^{\alpha_2 t})^2}{2 \left[ (\eta_1 + \eta_2 (a_0 t^{\alpha_1} e^{\alpha_2 t})) \ln(\eta_1 + \eta_2 (a_0 t^{\alpha_1} e^{\alpha_2 t})) \right]^2} \right) \right\} \end{aligned}$$

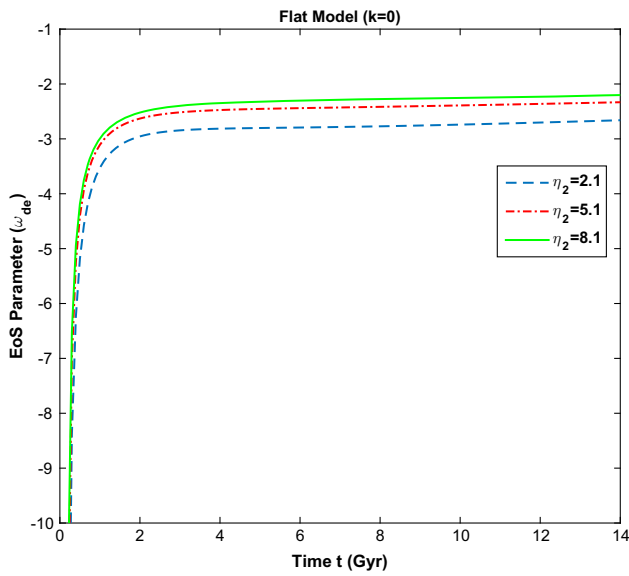


Fig. 21 Plot of EoS parameter versus cosmic time  $t$  in flat Model 2

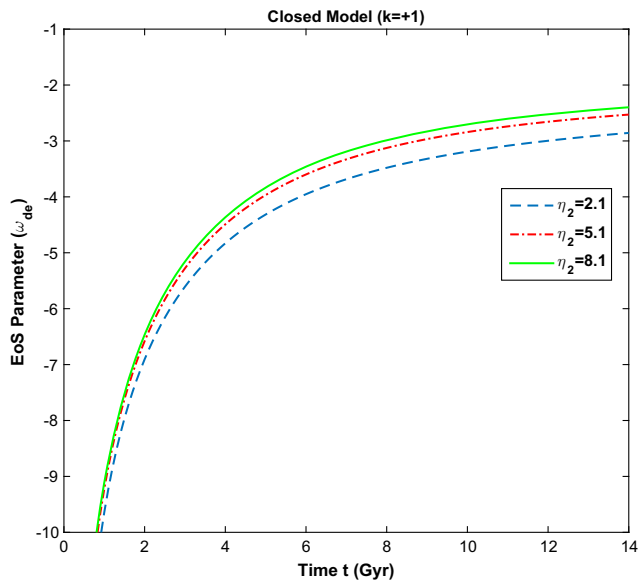


Fig. 22 Plot of EoS parameter versus cosmic time  $t$  in closed Model 2

$$+ \frac{6k}{(a_0 t^{\alpha_1} e^{\alpha_2 t})^2} \left\} - 3 \left\{ \beta_1 \left( \frac{\alpha_1}{t} + \alpha_2 \right) - \frac{\beta_2 \alpha_1}{t^2} + \frac{2\beta_3 \alpha_1}{3t^2(\alpha_1 + \alpha_2 t)} \right\}, \quad (33)$$

$$\Omega_k = \frac{\rho_k}{3\phi H^2} = \frac{kt^2}{(a_0 t^{\alpha_1} e^{\alpha_2 t})^2 (\alpha_1 + \alpha_2 t)^2}. \quad (34)$$

It can be seen from the Figs. 23, 24 that the behavior of overall energy density parameters of both models is similar to the case of Model 1.

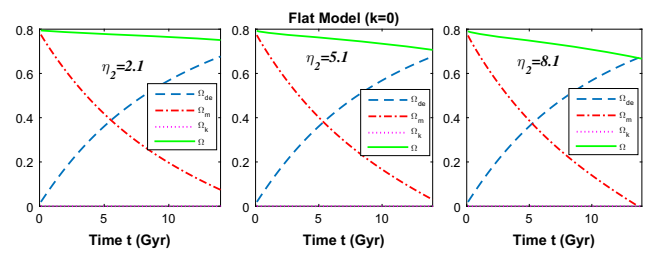


Fig. 23 Plot of density parameters versus cosmic time  $t$  in flat Model 2

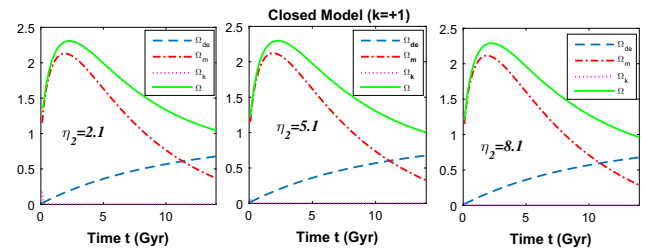


Fig. 24 Plot of density parameters versus cosmic time  $t$  in closed Model 2

### 3.2.5 Stability analysis

The squared sound speed  $v_s^2$  of MHRDE Model 2 is given by

$$v_s^2 = \left\{ - \frac{\phi_1}{24 \eta_1 + 24 \eta_2 a_0 t^{\alpha_1} e^{\alpha_2 t}} \left\{ \frac{\eta_2 a_0 t^{\alpha_1} \alpha_1 e^{\alpha_2 t}}{t} + \eta_2 a_0 t^{\alpha_1} \alpha_2 e^{\alpha_2 t} \right\} \left\{ \frac{3}{a_0 t^{\alpha_1} e^{\alpha_2 t}} \left\{ \frac{a_0 t^{\alpha_1} \alpha_1^2 e^{\alpha_2 t}}{t^2} - \frac{a_0 t^{\alpha_1} \alpha_1 e^{\alpha_2 t}}{t^2} + \frac{2a_0 t^{\alpha_1} \alpha_1 \alpha_2 e^{\alpha_2 t}}{t} + a_0 t^{\alpha_1} \alpha_2^2 e^{\alpha_2 t} \right\} + 3 \frac{1}{a_0^2 t^{2\alpha_1} e^{2\alpha_2 t}} \left\{ \frac{a_0 t^{\alpha_1} \alpha_1 e^{\alpha_2 t}}{t} + a_0 t^{\alpha_1} \alpha_2 e^{\alpha_2 t} \right\}^2 + 3 \frac{k}{a_0^2 t^{2\alpha_1} e^{2\alpha_2 t}} + \frac{w}{2} (\eta_1 + \eta_2 a_0 t^{\alpha_1} e^{\alpha_2 t})^{-2} \times \left\{ \ln (\eta_1 + \eta_2 a_0 t^{\alpha_1} e^{\alpha_2 t}) \right\}^{-2} \left\{ \frac{\eta_2 a_0 t^{\alpha_1} \alpha_1 e^{\alpha_2 t}}{t} + \eta_2 a_0 t^{\alpha_1} \alpha_2 e^{\alpha_2 t} \right\}^2 + (\eta_1 + \eta_2 a_0 t^{\alpha_1} e^{\alpha_2 t})^{-1} \times \left\{ a_0 t^{\alpha_1} e^{\alpha_2 t} \ln (\eta_1 + \eta_2 a_0 t^{\alpha_1} e^{\alpha_2 t}) \right\}^{-1} \left\{ \frac{a_0 t^{\alpha_1} \alpha_1 e^{\alpha_2 t}}{t} + a_0 t^{\alpha_1} \alpha_2 e^{\alpha_2 t} \right\} \left\{ \frac{\eta_2 a_0 t^{\alpha_1} \alpha_1 e^{\alpha_2 t}}{t} + \eta_2 a_0 t^{\alpha_1} \alpha_2 e^{\alpha_2 t} \right\} + \frac{1}{\phi_1 \ln (\eta_1 + \eta_2 a_0 t^{\alpha_1} e^{\alpha_2 t})} \left\{ \frac{\phi_1}{\eta_1 + \eta_2 a_0 t^{\alpha_1} e^{\alpha_2 t}} \times \left\{ \frac{\eta_2 a_0 t^{\alpha_1} \alpha_1^2 e^{\alpha_2 t}}{t^2} - \frac{\eta_2 a_0 t^{\alpha_1} \alpha_1 e^{\alpha_2 t}}{t^2} + \eta_2 a_0 t^{\alpha_1} \alpha_2^2 e^{\alpha_2 t} + \frac{2\eta_2 a_0 t^{\alpha_1} \alpha_1 \alpha_2 e^{\alpha_2 t}}{t} \right\} - \frac{\phi_1}{(\eta_1 + \eta_2 a_0 t^{\alpha_1} e^{\alpha_2 t})^2} \right.$$



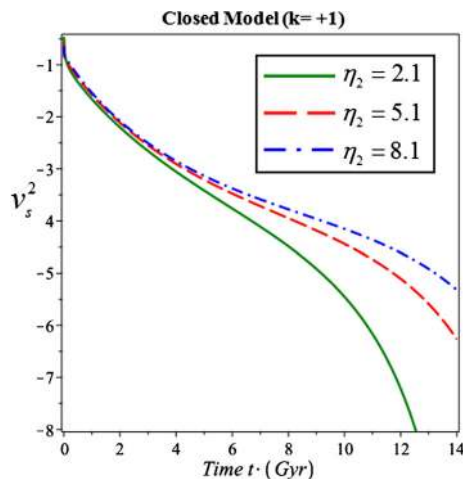


Fig. 25 Plot of  $v_s^2$  versus cosmic time  $t$  for closed Model 2

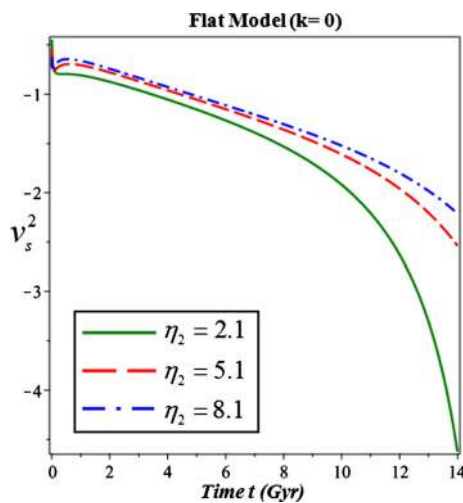


Fig. 26 Plot of  $v_s^2$  versus cosmic time  $t$  for flat Model 2

$$\begin{aligned}
 & \left. \frac{\phi_1 \left\{ \frac{\eta_2 a_0 t^{\alpha_1} \alpha_1 e^{\alpha_2 t}}{t} + \eta_2 a_0 t^{\alpha_1} \alpha_2 e^{\alpha_2 t} \right\}^2}{(\eta_1 + \eta_2 a_0 t^{\alpha_1} e^{\alpha_2 t})^2} \right\} \left\{ \frac{\eta_2 a_0 t^{\alpha_1} \alpha_1 e^{\alpha_2 t}}{t} \right. \\
 & \left. + \eta_2 a_0 t^{\alpha_1} \alpha_2 e^{\alpha_2 t} \right\} \left\{ \frac{\phi_1}{8 \eta_1 + 8 \eta_2 a_0 t^{\alpha_1} e^{\alpha_2 t}} \left\{ \frac{\eta_2 a_0 t^{\alpha_1} \alpha_1 e^{\alpha_2 t}}{t} \right. \right. \\
 & \left. \left. + \eta_2 a_0 t^{\alpha_1} \alpha_2 e^{\alpha_2 t} \right\} \left\{ \beta_1 \left\{ \frac{\alpha_1}{t} + \alpha_2 \right\} + \frac{2\beta_3 \alpha_1}{t^3} \left\{ \frac{\alpha_1}{t} + \alpha_2 \right\}^{-1} \right. \right. \\
 & \left. \left. - \frac{\beta_2 \alpha_1}{t^2} \right\} + 1/8 \phi_1 \ln(\eta_1 + \eta_2 a_0 t^{\alpha_1} e^{\alpha_2 t}) \left\{ -\frac{\beta_1 \alpha_1}{t^2} \right. \right. \\
 & \left. \left. + \frac{2\beta_2 \alpha_1}{t^3} + \frac{2\beta_3 \alpha_1^2}{t^5} \left\{ \frac{\alpha_1}{t} + \alpha_2 \right\}^{-2} \right. \right. \\
 & \left. \left. - \frac{6\beta_3 \alpha_1}{t^4} \left\{ \frac{\alpha_1}{t} + \alpha_2 \right\}^{-1} \right\} \right\}^{-1}. \tag{35}
 \end{aligned}$$

For different values of  $\eta_2$  the squared sound speed ( $v_s^2$ ) is shown in Figs. 25, 26, which show that both models are quite unstable.

### 3.2.6 $\omega_{de}-\omega'_{de}$ plane

In this case,  $\omega'_{de}$  is obtained by taking the derivative of Eq. (32) with respect to  $\ln a$ ,

$$\begin{aligned}
 \omega'_{de} = & \frac{8}{\phi_1 \ln(\eta_1 + \eta_2 a_0 t^{\alpha_1} e^{\alpha_2 t})} \left\{ -\frac{\phi_1}{24 \eta_1 + 24 \eta_2 a_0 t^{\alpha_1} e^{\alpha_2 t}} \right. \\
 & \times \left\{ \frac{\eta_2 a_0 t^{\alpha_1} \alpha_1 e^{\alpha_2 t}}{t} + \eta_2 a_0 t^{\alpha_1} \alpha_2 e^{\alpha_2 t} \right\} \left\{ 3 \frac{1}{a_0 t^{\alpha_1} e^{\alpha_2 t}} \right. \\
 & \times \left\{ \frac{a_0 t^{\alpha_1} \alpha_1^2 e^{\alpha_2 t}}{t^2} - \frac{a_0 t^{\alpha_1} \alpha_1 e^{\alpha_2 t}}{t^2} + \frac{2a_0 t^{\alpha_1} \alpha_1 \alpha_2 e^{\alpha_2 t}}{t} \right. \\
 & \left. \left. + a_0 t^{\alpha_1} \alpha_2^2 e^{\alpha_2 t} \right\} + \frac{3}{a_0^2 t^{2\alpha_1} e^{2\alpha_2 t}} \left\{ \frac{a_0 t^{\alpha_1} \alpha_1 e^{\alpha_2 t}}{t} \right. \right. \\
 & \left. \left. + a_0 t^{\alpha_1} \alpha_2 e^{\alpha_2 t} \right\}^2 + \frac{3k}{a_0^2 t^{2\alpha_1} e^{2\alpha_2 t}} + \frac{w}{2} (\eta_1 + \eta_2 a_0 t^{\alpha_1} e^{\alpha_2 t})^{-2} \right. \\
 & \times \left\{ \ln(\eta_1 + \eta_2 a_0 t^{\alpha_1} e^{\alpha_2 t}) \right\}^{-2} \left\{ \frac{\eta_2 a_0 t^{\alpha_1} \alpha_1 e^{\alpha_2 t}}{t} \right. \\
 & \left. \left. + \eta_2 a_0 t^{\alpha_1} \alpha_2 e^{\alpha_2 t} \right\}^2 + 3 \left\{ a_0 t^{\alpha_1} e^{\alpha_2 t} \ln(\eta_1 + \eta_2 a_0 t^{\alpha_1} e^{\alpha_2 t}) \right\}^{-1} \right. \\
 & \times (\eta_1 + \eta_2 a_0 t^{\alpha_1} e^{\alpha_2 t})^{-1} \left\{ \frac{a_0 t^{\alpha_1} \alpha_1 e^{\alpha_2 t}}{t} + a_0 t^{\alpha_1} \alpha_2 e^{\alpha_2 t} \right\} \\
 & \times \left\{ \frac{\eta_2 a_0 t^{\alpha_1} \alpha_1 e^{\alpha_2 t}}{t} + \eta_2 a_0 t^{\alpha_1} \alpha_2 e^{\alpha_2 t} \right\} \\
 & \left. + \frac{1}{\phi_1 \ln(\eta_1 + \eta_2 a_0 t^{\alpha_1} e^{\alpha_2 t})} \left\{ \frac{\phi_1}{\eta_1 + \eta_2 a_0 t^{\alpha_1} e^{\alpha_2 t}} \right. \right. \\
 & \times \left\{ \frac{\eta_2 a_0 t^{\alpha_1} \alpha_1^2 e^{\alpha_2 t}}{t^2} - \frac{\eta_2 a_0 t^{\alpha_1} \alpha_1 e^{\alpha_2 t}}{t^2} \right. \\
 & \left. \left. + \frac{2\eta_2 a_0 t^{\alpha_1} \alpha_1 \alpha_2 e^{\alpha_2 t}}{t} + \eta_2 a_0 t^{\alpha_1} \alpha_2^2 e^{\alpha_2 t} \right\} \right. \\
 & \left. - \frac{\phi_1}{(\eta_1 + \eta_2 a_0 t^{\alpha_1} e^{\alpha_2 t})^2} \left\{ \frac{\eta_2 a_0 t^{\alpha_1} \alpha_1 e^{\alpha_2 t}}{t} \right. \right. \\
 & \left. \left. + \eta_2 a_0 t^{\alpha_1} \alpha_2 e^{\alpha_2 t} \right\}^2 \right\} - \frac{\phi_1}{24} \ln(\eta_1 + \eta_2 a_0 t^{\alpha_1} e^{\alpha_2 t}) \\
 & \times \left\{ \frac{3}{a_0 t^{\alpha_1} e^{\alpha_2 t}} \left\{ \frac{a_0 t^{\alpha_1} \alpha_1^3 e^{\alpha_2 t}}{t^3} - \frac{3a_0 t^{\alpha_1} \alpha_1^2 e^{\alpha_2 t}}{t^3} \right. \right. \\
 & \left. \left. + \frac{3a_0 t^{\alpha_1} \alpha_1^2 \alpha_2 e^{\alpha_2 t}}{t^2} + \frac{2a_0 t^{\alpha_1} \alpha_1 e^{\alpha_2 t}}{t^3} - \frac{3a_0 t^{\alpha_1} \alpha_1 \alpha_2 e^{\alpha_2 t}}{t^2} \right. \right. \\
 & \left. \left. + \frac{3a_0 t^{\alpha_1} \alpha_1 \alpha_2^2 e^{\alpha_2 t}}{t} + a_0 t^{\alpha_1} \alpha_2^3 e^{\alpha_2 t} \right\} - 3 \frac{\alpha_1}{a_0 t^{\alpha_1} e^{\alpha_2 t} t} \right. \\
 & \times \left\{ \frac{a_0 t^{\alpha_1} \alpha_1^2 e^{\alpha_2 t}}{t^2} - \frac{a_0 t^{\alpha_1} \alpha_1 e^{\alpha_2 t}}{t^2} + \frac{2a_0 t^{\alpha_1} \alpha_1 \alpha_2 e^{\alpha_2 t}}{t} \right. \\
 & \left. \left. + a_0 t^{\alpha_1} \alpha_2^2 e^{\alpha_2 t} \right\} - \frac{3\alpha_2}{a_0 t^{\alpha_1} e^{\alpha_2 t}} \left\{ \frac{a_0 t^{\alpha_1} \alpha_1^2 e^{\alpha_2 t}}{t^2} \right. \right. \\
 & \left. \left. - \frac{a_0 t^{\alpha_1} \alpha_1 e^{\alpha_2 t}}{t^2} + \frac{2a_0 t^{\alpha_1} \alpha_1 \alpha_2 e^{\alpha_2 t}}{t} + a_0 t^{\alpha_1} \alpha_2^2 e^{\alpha_2 t} \right\} \right. \\
 & \left. + 6 \frac{1}{a_0^2 t^{2\alpha_1} e^{2\alpha_2 t}} \left\{ \frac{a_0 t^{\alpha_1} \alpha_1 e^{\alpha_2 t}}{t} + a_0 t^{\alpha_1} \alpha_2 e^{\alpha_2 t} \right\} \right\}
 \end{aligned}$$



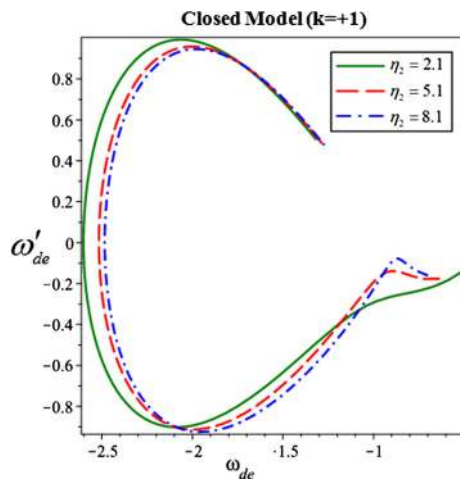


Fig. 27 Plot of  $\omega_{de}-\omega'_{de}$  plane of closed Model 2

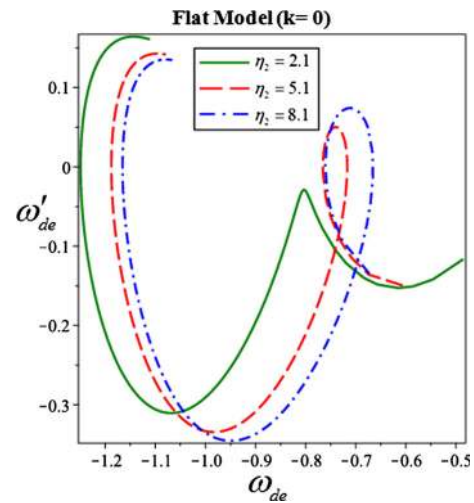


Fig. 28 Plot of  $\omega_{de}-\omega'_{de}$  plane of flat Model 2

$$\begin{aligned}
 & \times (a_0 t^{\alpha_1} e^{\alpha_2 t} \ln(\eta_1 + \eta_2 a_0 t^{\alpha_1} e^{\alpha_2 t}))^{-1} \left\{ \frac{a_0 t^{\alpha_1} \alpha_1 e^{\alpha_2 t}}{t} \right. \\
 & + a_0 t^{\alpha_1} \alpha_2 e^{\alpha_2 t} \left. \left\{ \frac{\eta_2 a_0 t^{\alpha_1} \alpha_1 e^{\alpha_2 t}}{t} + \eta_2 a_0 t^{\alpha_1} \alpha_2 e^{\alpha_2 t} \right\} \right. \\
 & + \frac{1}{\phi_1 \ln(\eta_1 + \eta_2 a_0 t^{\alpha_1} e^{\alpha_2 t})} \left\{ \frac{\phi_1}{\eta_1 + \eta_2 a_0 t^{\alpha_1} e^{\alpha_2 t}} \right. \\
 & \times \left\{ \frac{\eta_2 a_0 t^{\alpha_1} \alpha_1^2 e^{\alpha_2 t}}{t^2} - \frac{\eta_2 a_0 t^{\alpha_1} \alpha_1 e^{\alpha_2 t}}{t^2} \right. \\
 & + \left. \left. \frac{2\eta_2 a_0 t^{\alpha_1} \alpha_1 \alpha_2 e^{\alpha_2 t}}{t} + \eta_2 a_0 t^{\alpha_1} \alpha_2^2 e^{\alpha_2 t} \right\} \right. \\
 & - \frac{\phi_1}{(\eta_1 + \eta_2 a_0 t^{\alpha_1} e^{\alpha_2 t})^2} \left\{ \frac{\eta_2 a_0 t^{\alpha_1} \alpha_1 e^{\alpha_2 t}}{t} \right. \\
 & + \left. \left. \eta_2 a_0 t^{\alpha_1} \alpha_2 e^{\alpha_2 t} \right\}^2 \right\} \left\{ \frac{\phi_1}{8\eta_1 + 8\eta_2 a_0 t^{\alpha_1} e^{\alpha_2 t}} \right. \\
 & \times \left. \left. \left\{ \frac{\eta_2 a_0 t^{\alpha_1} \alpha_1 e^{\alpha_2 t}}{t} + \eta_2 a_0 t^{\alpha_1} \alpha_2 e^{\alpha_2 t} \right\} \left\{ \beta_1 \left\{ \frac{\alpha_1}{t} + \alpha_2 \right\} \right. \right. \right. \\
 & - \left. \left. \frac{\beta_2 \alpha_1}{t^2} + \frac{2\beta_3 \alpha_1}{t^3} \left\{ \frac{\alpha_1}{t} + \alpha_2 \right\}^{-1} \right\} \right. \\
 & + \left. \frac{\phi_1}{8} \ln(\eta_1 + \eta_2 a_0 t^{\alpha_1} e^{\alpha_2 t}) \right. \\
 & \times \left. \left. \left\{ -\frac{\beta_1 \alpha_1}{t^2} + \frac{2\beta_2 \alpha_1}{t^3} + \frac{2\beta_3 \alpha_1^2}{t^5} \left\{ \frac{\alpha_1}{t} + \alpha_2 \right\}^{-2} \right. \right. \right. \\
 & - \left. \left. \frac{6\beta_3 \alpha_1}{t^4} \left\{ \frac{\alpha_1}{t} + \alpha_2 \right\}^{-1} \right\} \right\} \left\{ 3\beta_1 \left\{ \frac{\alpha_1}{t} + \alpha_2 \right\} \right. \\
 & - \left. \left. \frac{3\beta_2 \alpha_1}{t^2} + \frac{6\beta_3 \alpha_1}{t^3} \left\{ \frac{\alpha_1}{t} + \alpha_2 \right\}^{-1} \right\}^{-1} \right\} \left\{ \frac{\alpha_1}{t} + \alpha_2 \right\}^{-1} \\
 & \times \left. \left. \left\{ \beta_1 \left\{ \frac{\alpha_1}{t} + \alpha_2 \right\} - \frac{\beta_2 \alpha_1}{t^2} + \frac{2\beta_3 \alpha_1}{t^3} \left\{ \frac{\alpha_1}{t} + \alpha_2 \right\}^{-1} \right\}^{-1} \right. \right. \\
 & \left. \left. \right. \right. \quad (36)
 \end{aligned}$$

The cosmological  $\omega_{de}-\omega'_{de}$  plane of Model 2 for different values of  $\eta_2$  is given in Figs. 27–28. It is observed that for both models it lies in both thawing and freezing regions.

#### 4 Some other properties of the models

Spatial volume of the models as

$$V = (a_1 t^{\alpha_1} e^{\alpha_2 t})^4. \tag{37}$$

The Hubble parameter is

$$H = \frac{\alpha_1}{t} + \alpha_2. \tag{38}$$

The scalar expansion is

$$\theta = 4 \left( \frac{\alpha_1}{t} + \alpha_2 \right). \tag{39}$$

The deceleration parameter is

$$q = -1 + \frac{\alpha_1}{(\alpha_1 + \alpha_2 t)^2}. \tag{40}$$

Many DE models have been proposed to explain the accelerated expansion phenomenon of the universe. In order to verify the viability of these models, Sahni et al. [72] have proposed the statefinder parameters  $(r, s)$ . The cosmological plane corresponding to these parameters is named the  $r-s$  plane; it explains the distance of a given DE model from the  $\Lambda$ CDM limit. The cosmological plane of these parameters describes different well-known regions of the universe; i.e.,  $s > 0$  and  $r < 1$  gives the region of phantom and quintessence DE eras,  $(r, s) = (1, 0)$  corresponds to the  $\Lambda$ CDM limit,  $(r, s) = (1, 1)$  represents the CDM limit, and  $s < 0$  and  $r > 1$  indicate the Chaplygin gas. The statefinder parameters for our models are given by



$$r = \frac{\ddot{a}}{aH^3} = 1 + \frac{2\alpha_1}{(\alpha_1 + t\alpha_2)^3} - \frac{3\alpha_1}{(\alpha_1 + t\alpha_2)^2}, \tag{41}$$

$$s = \frac{r - 1}{3(q - \frac{1}{2})} = \frac{2\alpha_1[2 - 3(\alpha_1 + \alpha_2 t)]}{3(\alpha_1 + \alpha_2 t)(\alpha_1 - 3(\alpha_1 + \alpha_2 t)^2)}. \tag{42}$$

Figure 29 shows the behavior of the deceleration parameter against cosmic time  $t$ . It can be observed that our models exhibit a smooth transition from early deceleration ( $q > 0$ ) to the present acceleration ( $q < 0$ ) phase of the universe. Also it may be noted that the present value (i.e., at  $t_0 = 13.7$  Gyr) of the deceleration parameter is  $q_0 = -0.73$  (Cunha [73]) and is approaching the value  $-1$  at late times. Recent observational data of SNe Ia shows that the present universe is accelerating with the value of the deceleration parameter lying in the range  $-1 \leq q < 0$ . The statefinder plane can be obtained by plotting  $r$  versus  $s$  as shown in Fig. 30. It is pointed out that the  $r$ - $s$  plane for Model 1 and Model 2 possess the regions of the quintessence and phantom models. We also observe that our models correspond to  $\Lambda$ CDM limit at late times.

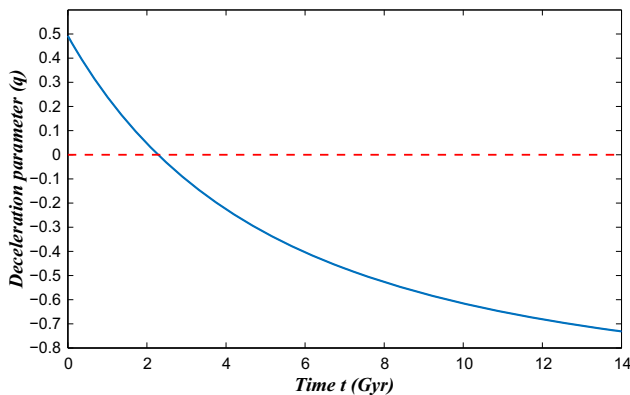


Fig. 29 Plot of deceleration parameter versus time  $t$  for  $\alpha_1 = 0.67$  and  $\alpha_2 = 0.065$

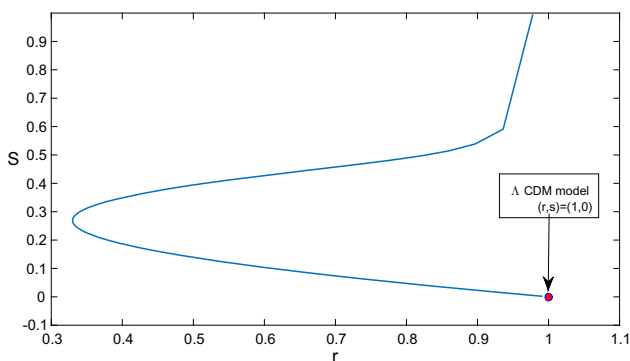


Fig. 30 Plot of  $r$ - $s$  plane for  $\alpha_1 = 0.67$  and  $\alpha_2 = 0.065$

### 5 Conclusions and discussion

The scalar-tensor theory of gravitation proposed by Brans and Dicke plays a significant role in the discussion of dark energy cosmology. Hence, in this paper, by solving the BD field equations we have obtained Kaluza-Klein FRW cosmological models filled with baryonic matter and MHRDE. We observed that the volumes of Model 1 and Model 2 increase with time, and Hubble’s parameter ( $H$ ) and expansion scalar ( $\theta$ ) become constant at late times showing a uniform spatial expansion of the universe.

The physical behavior of the cosmological parameters is studied through their graphical representation. Here we have two interesting models corresponding to the two forms of the BD scalar field. The following are the interesting observations in the two models:

#### Model 1

- Here the flat and closed FRW models are realistic because of the fact that the energy densities of matter  $\rho_m$  and MHRDE  $\rho_{de}$  are always positive and decrease with cosmic time (Figs. 2, 3, 4). Further, in the above realistic models, the interesting fact is that  $\rho_m$  dominates  $\rho_{de}$  initially and  $\rho_{de}$  dominates  $\rho_m$  later.
- It is observed that the scalar field increases with time for the three values of  $l = 0.1, 0.5, 0.9$  (Fig. 1). Also, it is interesting to note that as the BD scalar field increases the dominance of either matter energy density or the MHRDE density is delayed considerably.
- If we observe the energy conditions of the model we may notice that the NEC, SEC, and WEC are initially satisfied and are violated at late times. This is because of the fact that the universe is accelerating, which is in accordance with the recent observational data (Figs. 5, 6).
- The behavior of EoS parameter shows that the flat model starts in the matter dominated era and attains a constant value in the quintessence region for  $l = 0.1$  and  $0.5$ . Also, the flat model crosses the phantom divide line ( $\omega_{de} = -1$ ) and enters into the phantom region for  $l = 0.9$ . It is interesting to note that as the BD scalar field increases the flat model approaches the phantom region (Fig. 7). In the closed model it can be observed that the model completely varies in the phantom region and approaches  $\Lambda$ CDM model at late times (Fig. 8). We also found that  $\omega_{de}$  of our closed and flat models meet the ranges  $-1.13^{+0.24}_{-0.25}$  (Planck+WP+BAO) and  $-1.09 \pm 0.17$  (Planck+WP+Union 2.1) given by Ade et al. [74] (Planck data). This shows the consistency of our results with the recent observations.
- The study of the overall density parameter shows that it is constant and  $\approx 1$ , which is in agreement with the observational data. It is observed that the matter energy density

parameter,  $\Omega_m$ , initially dominates the overall density of dark energy and they interact at a certain point of time. That is, the BD scalar field  $\phi$  influences the interaction of energy densities (Figs. 9 and 10). It is well known that dark energy does not directly interact with visible matter except in the rare circumstances. It is quite interesting that in our case both of them interact at a certain point of time.

- It is observed from the stability analysis of the model that the closed and flat models are mostly unstable, which should be the case in the present scenario. We have observed that in this case also the BD scalar field influences the stability of the models (Figs. 11 and 12). It can be noted from the  $\omega_{de}-\omega'_{de}$  analysis that the models vary in both the thawing and the freezing regions (Fig. 13 and 14).
- The behavior of DP shows that the models exhibit a smooth transition of the universe from early deceleration phase to the present accelerated phase. The present value of the deceleration parameter is  $q_0 \approx -0.73$  (Fig. 29). It is observed from the  $r-s$  trajectory that the models correspond to  $\Lambda$ CDM limit (Fig. 30). Also, the trajectories coincide with the quintessence and phantom regions.

## Model 2

- In this case, the behavior of BD scalar field is discussed for different values of  $\eta_2$  (Fig. 15). We have observed that the scalar field increases as  $\eta_2$  increases. The study of the energy densities for this model (both flat and closed models) has shown that a similar behavior as in the Model 1 (Figs. 16, 17, 18). We also noticed that the increase in the BD scalar field influences the interaction of energy densities.
- We observe that the energy conditions of both closed and flat models in this case are also violated, which is similar to that of the energy conditions of Model 1 (Figs. 19 and 20). It is observed that the behavior of the overall energy density parameters of both models (closed and flat) is similar to the case of Model 1 (Figs. 23, 24).
- The behavior of the EoS parameter shows that both models (closed and flat) completely lie in the phantom region (Figs. 21 and 22). This shows that Model 2 supports the pilgrim DE phenomenon.
- From the stability analysis of both models we observe that they are unstable (Figs. 25 and 26). The  $\omega_{de}-\omega'_{de}$  plane lies in both the thawing and the freezing regions (Figs. 27 and 28).

Now it will be interesting to compare Model 1 and 2 with regard to the energy densities, the EoS parameter, the stability analysis, and the cosmological planes. It is observed that as the BD scalar field increases, in Model 1, the interaction of

the energy densities is delayed as compared to Model 2. In Model 1 the EoS parameter of the flat model shows that it lies in the quintessence region, while in the closed model the EoS parameter shows that the model varies in the phantom region and approaches the  $\Lambda$ CDM model. But, in Model 2, the EoS parameter shows that both (flat and closed) models (flat and closed) completely lie in the phantom region. However, the study of the deceleration parameter, the stability analysis, and the cosmological planes give us the same behavior in Model 1 and Model 2.

The above discussion shows that our models are in good agreement with the recent scenario of modern cosmology.

**Acknowledgements** We thank the reviewer for the positive and constructive comments, which have helped to improve the quality and presentation of the manuscript.

**Open Access** This article is distributed under the terms of the Creative Commons Attribution 4.0 International License (<http://creativecommons.org/licenses/by/4.0/>), which permits unrestricted use, distribution, and reproduction in any medium, provided you give appropriate credit to the original author(s) and the source, provide a link to the Creative Commons license, and indicate if changes were made. Funded by SCOAP<sup>3</sup>.

## References

1. A.G. Riess et al., *Astron. J.* **116**, 1009 (1998)
2. S. Perlmutter et al., *Astrophys. J.* **517**, 565 (1999)
3. C.L. Bennett et al., *Astrophys. J.* **583**, 1 (2003)
4. B. Ratra, J. Peebles, *Phys. Rev. D* **37**, 321 (1988)
5. R.R. Caldwell, *Phys. Lett. B* **545**, 23 (2002)
6. S. Nojiri, S.D. Odintsov, *Phys. Lett. B* **565**, 1 (2003)
7. T. Chiba et al., *Phys. Rev. D* **62**, 023511 (2000)
8. M.C. Bento et al., *Phys. Rev. D* **66**, 043507 (2002)
9. A.G. Cohen et al., *Phys. Rev. Lett.* **82**, 4971 (1999)
10. T. Padmanabhan, *Phys. Rep.* **380**, 235 (2003)
11. E.J. Copeland et al., *Int. J. Mod. Phys. D* **15**, 1753 (2006)
12. K. Bamba et al., *Astrophys. Space Sci.* **342**, 155 (2012)
13. M.R. Setare, *Phys. Lett. B* **642**, 1 (2006)
14. A. Sheykhi, *Phys. Lett. B* **680**, 113 (2009)
15. L. Susskind, *J. Math. Phys.* **36**, 6377 (1995)
16. A. Cohen, D. Kaplan, *Phys. Rev. Lett.* **82**, 4971 (1999)
17. M. Li, *Phys. Lett. B* **603**, 1 (2004)
18. C. Gao et al., *Phys. Rev. D* **79**, 043511 (2009)
19. Q.G. Huang, M. Li, *JCAP* **2004**, 013 (2004)
20. X. Zhang, F.Q. Wu, *Phys. Rev. D* **72**, 043524 (2005)
21. L.N. Granda, A. Oliveros, *Phys. Lett. B* **669**, 275 (2008)
22. S. Chen, J. Jing, *Phys. Lett. B* **679**, 144 (2009)
23. S. Sarkar, C.R. Mahanta, *Int. J. Theor. Phys.* **52**, 1482 (2013)
24. V.U.M. Rao, U.Y. Divya Prasanthi, *Afr. Rev. Phys.* **11**, 0001 (2016)
25. K.S. Adhav et al., *Astrophys. Space Sci.* **359**, 24 (2015)
26. M. Kiran et al., *Astrophys. Space Sci.* **354**, 2099 (2014)
27. M.V. Santhi et al., *Int. J. Theor. Phys.* **56**, 362 (2017)
28. K. Das, T. Sultana, *Astrophys. Space Sci.* **361**, 53 (2016)
29. M.V. Santhi et al., *Can. J. Phys.* **95**, 179 (2017)
30. V.U.M. Rao, U.Y.D. Prasanthi, *Eur. Phys. J. Plus* **132**, 64 (2017)
31. M.V. Santhi et al., *Astrophys. Space Sci.* **361**, 142 (2016)
32. M.V. Santhi et al., *Can. J. Phys.* **95**, 381 (2017)
33. C.H. Brans, R.H. Dicke, *Phys. Rev.* **124**, 925 (1961)
34. E. Witten, *Phys. Lett. B* **144**, 351 (1984)

35. T. Appelquist et al., *Modern Kaluza–Klein Theories* (Addison Wesley, Boston, 1987)
36. A. Chodos, S. Detwiler, Phys. Rev. D **21**, 2167 (1980)
37. S. Chatarjee et al., Phys. Lett. A **149**, 91 (1990)
38. S. Chatarjee, Ann. Phys. **218**, 121 (1992)
39. T. Kaluza, Zum Unitatsproblem der Physik Sitz. Press. Akad. Wiss. Phys. Math. k1, 966 (1921)
40. O. Klein, Zeits. Phys. **37**, 895 (1926)
41. C. Ozel et al., Adv. Stud. Theor. Phys. **4**, 117 (2010)
42. M. Sharif, F. Khanum, Astrophys. Space Sci. **334**, 209 (2011)
43. M. Sharif, A. Jawad, Eur. Phys. J. C **72**, 1901 (2012)
44. D.R.K. Reddy, R. Santhi Kumar, Astrophys. Space Sci. **349**, 485 (2014)
45. P.K. Sahoo et al., Indian J. Phys. **90**, 485 (2016)
46. O. Akarsu, C.B. Kilinc, Gen. Relativ. Gravit. **42**, 119 (2010)
47. A.K. Yadav, Astrophys. Space Sci. **335**, 565 (2011)
48. S. Kumar, C.P. Singh, Gen. Relativ. Gravit. **43**, 1427 (2011)
49. V.U.M. Rao et al., Astrophys. Space Sci. **337**, 499 (2012)
50. D.R.K. Reddy et al., Astrophys. Space Sci. **351**, 661 (2014)
51. O. Akarsu, JCAP **01**, 022 (2014)
52. Shri Ram, S. Chandell, Astrophys. Space Sci. **355**, 195 (2015)
53. V.B. Johri, K. Desikan, Gen. Relativ. Gravit. **26**, 1217 (1994)
54. V.B. Johri, R. Sudharsan, Aust. J. Phys. **42**, 215 (1989)
55. C.P. Singh, Astrophys. Space Sci. **338**, 411 (2012)
56. M.V. Santhi et al., Can. J. Phys. **94**, 578 (2016)
57. A. Sheykhi, Phys. Lett. B **681**, 205 (2009)
58. X.L. Liu, X. Zhang, Commun. Theor. Phys. **52**, 761 (2009)
59. S. Chattopadhyay et al., Eur. Phys. J. C **74**, 3080 (2014)
60. P. Kumar, C.P. Singh, Astrophys. Space Sci. **362**, 52 (2017)
61. C.P. Singh, P. Kumar, Int. J. Theor. Phys. **56**, 3297 (2017)
62. E. Sadri, B. Vakili, Astrophys. Space Sci. **363**, 13 (2018)
63. Y.S. Myung, Phys. Lett. B **652**, 223 (2007)
64. A. Jawad et al., Astrophys. Space Sci. **344**, 489 (2013)
65. A. Jawad, S. Chattopadhyay, Astrophys. Space Sci. **357**, 37 (2015)
66. R.R. Caldwell, E.V. Linder, Phys. Rev. Lett. **95**, 141301 (2005)
67. R.J. Scherrer, Phys. Rev. D **73**, 043502 (2006)
68. T. Chiba, Phys. Rev. D **73**, 063501 (2006)
69. M.R. Setare, J. Comput. Astropart. Phys. **03**, 007 (2007)
70. A. Jawad, Astrophys. Space Sci. **353**, 691 (2014)
71. M. Sharif, A. Jawad, Eur. Phys. J. C **73**, 2382 (2013)
72. V. Sahni et al., J. Exp. Theor. Phys. Lett. **77**, 201 (2003)
73. J.V. Cunha, Phys. Rev. D **79**, 047301 (2009)
74. P.A.R. Ade et al., A&A **571**, A1 (2014)